EPRI | ELECTRIC POWER RESEARCH INSTITUTE

Technical Reference on the Composite Load Model

3002019209

Technical Reference on the Composite Load Model

3002019209

Technical Update, September 2020

EPRI Project Manager

P. Mitra

ELECTRIC POWER RESEARCH INSTITUTE
3420 Hillview Avenue, Palo Alto, California 94304-1338 ▪ PO Box 10412, Palo Alto, California 94303-0813 ▪ USA
800.313.3774 ▪ 650.855.2121 ▪ askepri@epri.com ▪ www.epri.com

DISCLAIMER OF WARRANTIES AND LIMITATION OF LIABILITIES

This is an EPRI Technical Update report. A Technical Update report is intended as an informal report of continuing research, a meeting, or a topical study. It is not a final EPRI technical report.

NOTE

For further information about EPRI, call the EPRI Customer Assistance Center at 800.313.3774 or e-mail askepri@epri.com.

ACKNOWLEDGMENTS

The Electric Power Research Institute (EPRI) prepared this report.

Principal Investigators
P. Mitra
A. Gaikwad
D. Ramasubramanian
L. Sundaresh

This report describes research sponsored by EPRI. EPRI would like to acknowledge the support of the following organizations:

Ameren Services Co.
American Electric Power Service Corp.
CenterPoint Energy Houston Electric, LLC
CPS Energy
Dominion Energy, Inc.
Eskom Holdings SOC Limited
FirstEnergy Service Company
Great River Energy
Hoosier Energy Rural Electric Coop., Inc.
Hydro One Networks Inc.
Lincoln Electric System
Midcontinent Independent System Operator, Inc.
National Grid UK, Ltd.
Nebraska Public Power District
New York ISO
New York Power Authority
PJM Interconnection
Salt River Project Agricultural Improvement and Power District
Southern Company
Southwest Power Pool, Inc.
Tri-State Generation & Transmission Association, Inc.
Xcel Energy Services, Inc.

The project team would like to thank the following individuals for their feedback, reviews and comments:

Pouyan Pourbeik, *Power and Energy, Analysis, Consulting and Education (PEACE), PLLC*
Irina Green, *California Independent System Operator*
Dmitry Kosterev, *Bonneville Power Administration*

This publication is a corporate document that should be cited in the literature in the following manner:

Technical Reference on the Composite Load Model. EPRI, Palo Alto, CA: 2020. 3002019209.

ABSTRACT

This document serves as a technical reference document for load modeling and the composite load model. The document is intended to be used as a guide for transmission planners and utility engineers to understand and use the composite load model for transmission planning studies. The document is organized in 5 chapters.

Chapter 1 provides a brief introduction to the history of load modeling and summarizes the journey from basic ZIP models to the present composite load model. Chapter 2 provides a brief summary of the CLOD model, which was a predecessor to the latest composite load model. Chapter 3 provides a detailed summary of the WECC composite load model, also known simply as the composite load model. Chapter 4 provides a note on the practices and methods for composite load model parameterization. Finally, chapter 5 briefly summarizes some of the major research initiatives that are being pursued towards the improvement of the composite load model at the time of writing of this report. Additionally, the document contains an Appendix that lists some additional mathematical details about the individual components of the composite load model.

Keywords
Load modeling
Composite load model
Model parameterization
Transmission planning

CONTENTS

LIST OF FIGURES

LIST OF TABLES

1
A BRIEF HISTORY OF LOAD MODELING

The importance of proper representation of loads in power system studies has long been recognized. In the early days of power system simulation, simple load models were adopted, where the active power of loads was represented as constant current and the reactive power was represented as constant impedance [1]. This was done due to computational limitations. To enhance the simple load models, research conducted by EPRI in 1980s demonstrated the advantages of a component-based load modeling process [2,3,4]. Later, EPRI developed the LOADSYN software that could take in information about load class mix, load composition and load characteristics and construct a load model consisting of an algebraic constant impedance (Z), constant current (I), and constant power (P) component for use in power flow and transient stability studies. This structure is commonly referred to as the ZIP load model. Thus, utilities could develop a variety of static ZIP models to represent the diversity of loads in their footprint.

With advancements in computational technology, incorporation of dynamic load models became possible. In 1993, IEEE recommended the use of dynamic load models in power system stability studies [5] but the recommendation did not gain much traction till 1996. In 1996, model validation studies for July 2 and August 10, 1996 outages in the Western Electricity Coordinating Council (WECC) concluded that dynamic motor models were needed to capture the North-South power oscillations [6]. To address this, in 2001, WECC developed a model in which 20% of load was represented as induction motor load and the rest 80% was represented as static load. This load model representation was good enough to capture the power oscillations but was not realistic because the loads were aggregated at high-voltage buses (115 kV or 138 kV) without any representation of substation transformer and distribution feeder impedances. The interim load model was not able to capture the fault induced delayed voltage recovery (FIDVR) events that were observed in the Southern California and Florida. These FIDVR events were seen as reliability risks and needed to be captured in simulation studies. Thus, WECC set up the load modeling task force to develop a full-scale composite load model in 2002 [7]. By 2005, WECC developed a load model which included a distribution system equivalent and could be used in interconnection studies without numerical instability.

By 2007, a composite load model was developed based on the basic structure developed by Southern California Edison (SCE). This composite model included three different induction motor models that could be used to capture the response of diverse motor loads. However, this model excluded a representation of single-phase induction motor driven residential air-conditioning systems that were prone to stalling and primarily responsible for FIDVR. To address this shortcoming, the Electric Power Research Institute (EPRI), Bonneville Power Administration (BPA), and SCE conducted comprehensive tests on residential air conditioners at their lab facilities. The test results were used to develop a performance-based model of single-phase air conditioner and was completed in in 2009 [9]. After a series of system impact studies were conducted on the WECC system, the modeled was approved and formally included in the composite load model [10]. This version of the composite load model was commonly referred to as the WECC composite load model. The most recent addition to the composite load model is the

DER_A component [11], which is used to model the behind-the-meter distributed generation in the system.

References

[1] C. Concordia and S. Ihara, "Load Representation in Power System Stability Studies," in IEEE Transactions on Power Apparatus and Systems, vol. PAS-101, no. 4, pp. 969-977, April 1982, doi: 10.1109/TPAS.1982.317163.

[2] Gentile, T, Ihara, S, Murdoch, A, and Simons, N. "Determining load characteristics for transient performance". Volume 3. Load-composition data analysis. Final report. United States: N. p., 1981.

[3] EPRI Load Model Synthesis Program Package: Load Modeling Reference Manual, September 1986.

[4] W. W. Price, K. A. Wirgau, A. Murdoch, J. V. Mitsche, E. Vaahedi and M. El-Kady, "Load modeling for power flow and transient stability computer studies," *IEEE Transactions on Power Systems*, vol. 3, no. 1, pp. 180-187, Feb. 1988, doi: 10.1109/59.43196.

[5] IEEE Task Force on Load Representation for Dynamic Performance, "Load Representation for Dynamic Performance Analysis," *IEEE Transactions on Power Systems*, vol.8, no.2, May 1993, pp.472-482.

[6] D.N.Kosterev, C.W.Taylor, W.A.Mittelstadt, "Model Validation for the August 10, 1996 WSCC System Outage," *IEEE Transactions on Power Systems*, vol.14, no.3, pp.967-979, August 1999.

[7] Les Pereira, Dmitry Kosterev, Peter Mackin, Donald Davies, John Undrill, Wenchun Zhu, "An Interim Dynamic Induction Motor Model for Stability Studies in WSCC," *IEEE Transactions on Power Systems*, vol.17, no.4, November 2002, pp1108-1115.

[8] Dmitry Kosterev, Anatoliy Meklin , John Undrill, Bernard Lesieutre, William Price, David Chassin, Richard Bravo, Steve Yang, "Load Modeling in Power System Studies: WECC Progress Update", presented at 2008 *IEEE Power Engineering Society General Meeting*, Pittsburgh, PA.

[9] A.M.Gaikwad, Richard Bravo, D.Kosterev, S.Yang, A. Maitra, P.Pourbeik, B.Agrawal, R.Yinger, D, Brooks, "Results of Air-Conditioner Testing in WECC," *Power and Energy Society General Meeting* – Conversion and Delivery of Electrical Energy in the 21st Century, 2008 IEEE.

[10] North American Electric Reliability Corporation (NERC) Load Modeling Task Force," Dynamic load modeling Technical Reference Document", December 2016.

[11] EPRI Report, *A New Aggregated Distributed Energy Resources (DER_A) Model for Transmission Planning Studies*, Product ID: 3002013498, May 8, 2018.

2
THE COMPLEX LOAD MODEL

The complex load model or CLOD is often considered a predecessor of the composite load model and is still widely used by utilities within the United States as well as worldwide. Although the model is a significant development from the simple ZIP representation, it still lacks the capability to model events like FIDVR, which can have significant consequences on planning decisions. At present a significant number of utilities are transitioning from the CLOD model to the composite load model, and the North American Electricity Reliability Corporation's (NERC) load modeling task force is spearheading this effort. This chapter provides a very brief description of the CLOD model.

The CLOD Model

Complex load model (CLOD) was developed to capture the aggregate dynamic response of loads. This model is simple and requires far fewer computational resources than the composite load model. It is also useful when the comprehensive data about the load is not available for the composite load model. The basic structure of the model is shown in Figure 2-1.

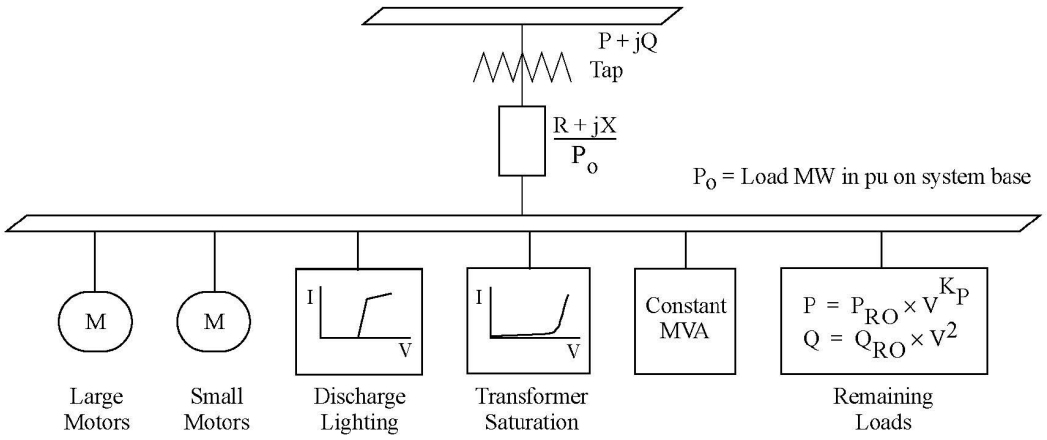

Figure 2-1
The CLOD model [1]

The CLOD structure includes a large induction motor, a small induction motor, discharge lighting, transformer saturation and static load models. The percentage of each of these components in the load can be changed based on the load mix it is being used to represent. The distribution transformer impedance can also be specified by the user. The CLOD model has the following features [1], [2]:

1. During initialization of this model, the tap on the distribution transformer is adjusted to maintain a voltage level of 0.98 pu at load end of the transformer.
2. The real power for each of the components is calculated based on the percentage specified by the user (except the transformer excitation current which does not include active power).

3. The reactive powers of the induction motors are calculated during model initialization.
4. The discharge lighting is assumed to have a power factor of 0.9, that is the reactive power is approximately 0.388 times the actual power consumed by the discharge lighting load.
5. The transformer excitation current is calculated based on the percentage specified by the user.
6. The static load is adjusted to match the reactive power load at the high side of the transformer. This is done to ensure that the reactive power at the high side matches with that in the power flow case.

The induction motor models have fixed parameters that are hard coded in the model and cannot be changed by the user. It is however important to note that the induction motor models used in Siemens PTI PSS®E and GE PSLF™ are different [2]. In GE PSLF™, the rotor flux dynamics as well as the mechanical dynamics are modeled with differential equations similar to that in the *motorw* model. In PSS®E however, only the mechanical dynamics of the induction motor models in CLOD are represented by differential equations. The flux dynamics are modeled using algebraic equations. Furthermore, in GE PSLF™ the mechanical torque is computed as [2]

$$\boldsymbol{T_m = T_{m0}\omega^D} \quad \text{(Eq. 1)}$$

whereas, in PSS®E the mechanical torque is linearly approximated as [2]

$$\boldsymbol{T_m = T_{m0}(1 + D\Delta\omega)} \quad \text{(Eq. 2)}$$

where D in (1) and (2) are the speed dependence factors of the driven loads.

The discharge lighting component is used to model mercury vapor lamps which are primarily used for outdoor lighting of public spaces [1], [2]. When the terminal voltage is above 0.75 pu, the discharge lighting is modeled as a constant current real part and an imaginary part proportional to the voltage raised to 4.5. When the voltage is in the 0.65 -0.75 pu range, the lighting load linearly decreases and finally trips as the voltage drops below 0.65 pu.

In addition to the load components, the CLOD model also has a representation of the distribution transformer. The transformation excitation characteristics is given by [2]

$$\begin{gathered} flux = V / (1 + \Delta f)\ [f = p.u.\ frequency] \\ Iexc = flux * 0.01 / 0.98\ if\ (flux \leq 0.98) \\ Iexc = 0.01 + (flux - 0.98) * (0.02 - 0.01) / (1.05 - 0.98)\ if\ (0.98 \leq flux \leq 1.0) \\ Iexc = 0.02 + (flux - 1.05) * (0.03 - 0.02) / (1.10 - 1.05)\ if\ (1.0 \leq flux \leq 1.1) \\ Iexc = 0.03 + (flux - 1.10) * (0.04 - 0.03) / (1.13 - 1.10)\ if\ (1.1 \leq flux) \\ Qexc = Iexc * V * Iexcbase \end{gathered} \quad \text{(Eq. 3)}$$

where,

$$Iexcbase = (Initial\ Qexc) * (initial\ Pload) / (0.01 * 0.98). \quad \text{(Eq. 4)}$$

References

[1] SIEMENS PTI PSS®E 33 Program Application Guide VOLUME 2, May 2016.

[2] GE PSLF™ User's Manual, 2019.

3
THE COMPOSITE LOAD MODEL

The composite load model (also known as the WECC composite load model) is the latest and the most updated dynamic load model available for use in all major power system simulation tools. Similar to its predecessor, the complex load model, this model represents an aggregation of consumer loads at the substation level. However, in contrast to the complex load model, the composite load model provides more flexibility in modeling the distribution feeder equivalent, as well as the diverse range of consumer load types. The composite load model can be used to model residential, commercial, and industrial loads for dynamic studies by making suitable changes to its parameters and structure.

The Composite Load Model Structure

The composite load model is available in all the most commonly used power system simulators such as:

A. Siemens PTI PSS®E [1]: the *CMLDXXU2* model

B. GE PSLF™ [2]: the *cmpldw* (and the *_cmpldw*) model

C. Powerworld Simulator [3]: can read both PSS®E (*.dyre*) and PSLF™ (*.dyd*) formats

D. PowerTech Labs DSATools [4]: can read both PSS®E (*.dyre*) and PSLF™ (*.dyd*) formats

Figure 3-1, shows the structure of the composite load model. The implementation of the composite load model may have slight differences across the different software platforms, however, conceptually the models are identical. Additionally, a series of rigorous benchmarking activities performed by different entities has confirmed that the response of the composite load model is essentially identical across major software platforms. The results of the benchmarking study can be found in [5], [6]. The composite load model consists of the following key components:

1. A distribution substation and feeder equivalent
2. Motor A: 3 phase induction motor driving a relatively low inertia, constant torque type load like positive displacement compressors and pumps
3. Motor B: 3 phase induction motor driving a relatively high inertia, variable torque type load like blower fans and large centrifugal compressors
4. Motor C: 3 phase induction motor driving a relatively low inertia, variable torque type load small centrifugal pumps
5. Motor D: A performance based algebraic model of a single-phase residential heat ventilation and air-conditioning (HVAC) system
6. Static load: The conventional constant impedance (Z), constant current (I) and constant power (P) model; and
7. Electronic load.

In addition to the detailed mathematical representation of the load components, the composite load model also has the provision for modeling the manufacturer installed equipment protection that consumer loads have. A detailed description of the composite load model along with the end uses that these components are intended to model is presented in this section.

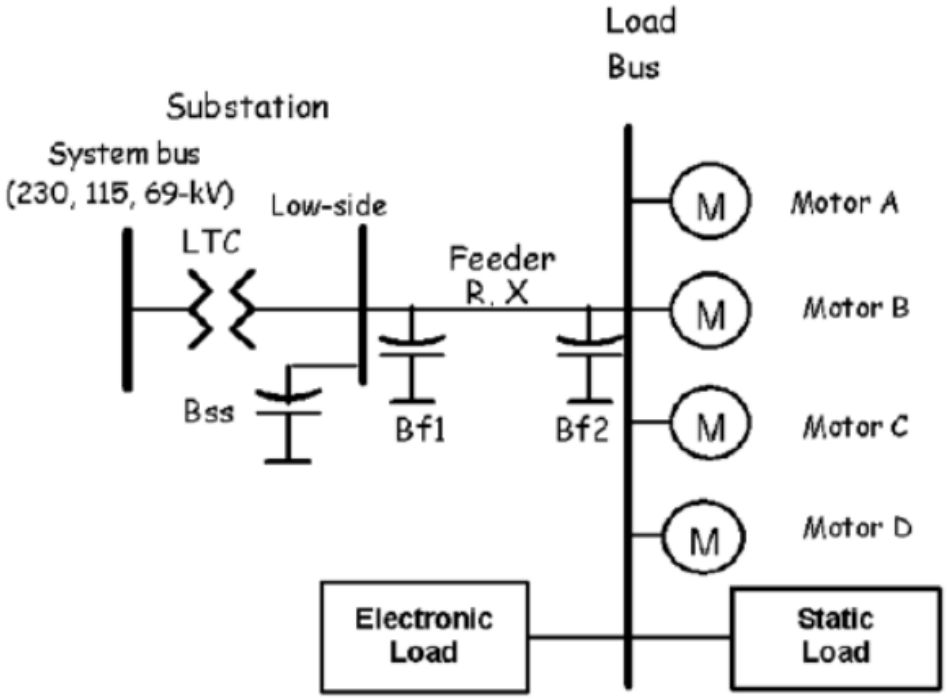

Figure 3-1
WECC Composite Load Model [2]

MVA rating and interpretation

When the composite load model data is supplied in a dynamic file (dyre or dyd) the MVA rating for the load record needs to be specified. It is important that the MVA base be specified properly since the per unit (pu) parameter values for the substation transformer and distribution feeder equivalent is set on this MVA base. An incorrect choice for the MVA base can result in unrealistic values of transformer and feeder impedance, causing issues with initialization and in some cases erroneous dynamic simulation results.

Typically, the choice of MVA base is guided by the MVA rating of the distribution transformer. Both dyd and dyre formats have two general options of specifying the MVA base for the load model [1], [2]:

1. **Actual MVA**: the user can supply the actual MVA rating of the aggregated load in the distribution feeder. E.g. the load at a load bus in the power flow file is 10 MW and a user specifies the MVA base as 12 MVA based on the knowledge of the substation transformer rating.

2. **Loading factor**: the user can choose to set a loading factor instead of an actual MVA rating. In this case, for the same 10 MW load at a load bus, a loading factor of 0.8 would indicate that the transformer and the feeder is rated as 10/0.8 =12.5 MVA. This condition indicates that the transformer is rated more than the actual load on that feeder for the snapshot being studied. Similarly, a loading factor of 1.25 would indicate that the transformer and is rated at 8 MVA, which indicates that the transformer is operating above its rating for that snapshot. Such a situation may be encountered when a distribution transformer has forced air cooling which allows them to operate above their ratings for a brief period of time.

In general, the loading factor is the preferred method of specifying the MVA base for load modeling. For the dyd and the dyre data formats a positive value for the MVA base is interpreted as the actual MVA, whereas a negative value for MVA base is treated as the loading factor. The readers are strongly encouraged to consult the relevant software user manuals for further guidance on specifying the MVA base appropriately.

The Substation and the Feeder Equivalent

The composite load model allows for the modeling of a distribution feeder equivalent to emulate the voltage regulation over a typical distribution feeder. Typical distribution feeders have a voltage regulation of 4 to 6% from the high side of the distribution transformer to the load terminals. A description of the substation and distribution feeder equivalent is as follows:

1. The distribution substation transformer: the distribution transformer is equipped with an on-load tap changer (OLTC) and can be used to regulate the low side voltage of the transformer both during model initialization and during the dynamic simulation [1, 2]. In case the distribution transformer is already modeled in the power flow case, the transformer impedance *Xxf* in the composite load model should be set to 0 and the transformed will be omitted.

2. The substation shunt capacitor: The composite load model has the option of modeling any shunt capacitors located at the distribution substation. This can be done by selecting an appropriate value for *Bss.*

3. The distribution feeder equivalent: The parameters *Rfdr* and *Xfdr* are used to model the equivalent distribution feeder. It is important to note that if the voltage at the load component terminals (refered to as load bus in Figure 3-1) is less than 0.95 pu during model initialization, the composite load model automatically adjusts the values of Rfdr and *Xfdr* to ensure that the voltage is greater than or equal to 0.95 pu. For voltages less than 0.95 pu, it is difficult to initialize the motor models in the composite load model. This adjustment is reasonable since the service voltage at the consumer terminal is expected to be within a ±5% range during normal steady state operation. In general, it is not recommended that the composite load model be added to load buses, where the voltages are below 0.95 pu in the powerflow. At such low voltages, the composite load model is difficult to initialize and may result in initialization errors.

When the composite load model is initialized, the active power of the motors and the static/electronic component is determined based on the percentages allocated to these components. The reactive power of the motors (motor A, B and C) are computed based on the calculated slip during initialization. The reactive power for Motor D, power electronic

component and the static (ZIP) model is computed based on the user specified power factor. It is possible that the total reactive power computed during initialization does not match with the load flow solution. In this case, a computed additional shunt capacitance, Bfdr, is added to the composite load model to account for this mismatch. Depending on the value of Fb, Bf1 (see Figure 3-1) is set to Fb*Bfdr and Bf2 (see Figure 3-1) is set to (1-Fb)*Bfdr. Table 3-1 lists the NERC recommended parameters for 5 different feeder types.

Table 3-1
NERC default feeder models for 5 different feeder types

	FDR_01	FDR_01_noLTC	FDR_02_CVR	FDR_02_noLTC	FDR_IND
Bss	0	0	0	0	0
Rfdr	0.04	0.04	0.04	0.04	0.02
Xfdr	0.04	0.04	0.04	0.04	0.02
Fb	0.75	0.75	0.75	0.75	1
Xxf	0.08	0.08	0.08	0.08	0.08
TfixHS	1	1	1	1	1
TfixLS	1	1	1	1	1
LTC	1	1	1	1	1
Tmin	0.9	0.9	0.9	0.9	0.9
Tmax	1.1	1.1	1.1	1.1	1.1
step	0.00625	0.00625	0.00625	0.00625	0.00625
Vmin	1.025	1.025	1	1	1
Vmax	1.04	1.04	1.02	1.02	1.02
Tdel	30	999	30	999	999
Ttap	5	5	5	5	5
Rcomp	0	0	0	0	0
Xcomp	0	0	0	0	0
Abbreviations					
FDR	Feeder				
LTC	Load Tap Changer				
CVR	Conservation Voltage Reduction				
IND	Industrial				

The Motor A Component

Motor A is used to represent an aggregation of 3-phase induction motors that drive low inertia constant torque loads. Typical examples of constant torque loads connected to a power system are:

1. positive displacement compressors (reciprocating, scroll, screw, rotary vane etc.)
2. positive displacement pumps

3. conveyors
4. hoists, etc.

Most commonly motor A is used to represent commercial HVAC compressors, that can be found in the rooftop air-conditioning units of grocery stores, small offices and businesses, malls and other large commercial buildings. Many large commercial buildings which have centralized air-conditioning systems also use positive displacement compressors. Most constant torque loads, due to the dimensions and design of the rotating parts, have a relatively low inertia.

Motors that run constant torque loads that require high starting torque. These types of loads are typically run using NEMA type A or type B motors, which are the most common NEMA motors in use. A large percentage of these loads are also run using special designed motors and thus may not fall precisely into the major NEMA categories. Realizing that all of the models in the composite load model are simply an aggregated behavior of a class of motors, the electrical characteristics of Motor A has been chosen to emulate a motor similar to the NEMA A category motors. Figure 3-2 shows the torque – slip characteristics of motor A for a terminal voltage of 1 pu and a terminal voltage of 0.5 pu. The black dotted line in Figure 3-2 shows the constant load torque line of 0.8 pu. From Figure 3-2 it can be seen that, for the shown motor, a steady state terminal voltage of 0.5 pu the motor A produces a steady state locked rotor torque equal to the load torque of 0.8 pu. This implies that the motor should theoretically be able to reaccelerate if a *stiff* terminal voltage of more than 0.5 pu is applied. This type of starting behavior is typical for NEMA type D motors.

Table 3-2 lists the NERC recommended parameters for motor A when used to model commercial low inertia constant torque loads. Table 3-3 lists the NERC recommended parameters when motor A is used for industrial low inertia constant torque loads. Based on industry experience, an inertia constant (H) of 0.1s is recommended for modeling these loads. This inertia constant in reflected in the motor A parameters listed in Table 3-2 and Table 3-3. Additionally, the parameter LF shown in Table 3-2 and Table 3-3 indicates the loading factor of the motor. A loading factor of 0.75 indicates that if the amount of load assigned to motor A is X MW during initialization, the MVA base for motor A will be X/0.75 = 1.33X MVA. The interpretation of the loading factor is same for all load components, wherever applicable.

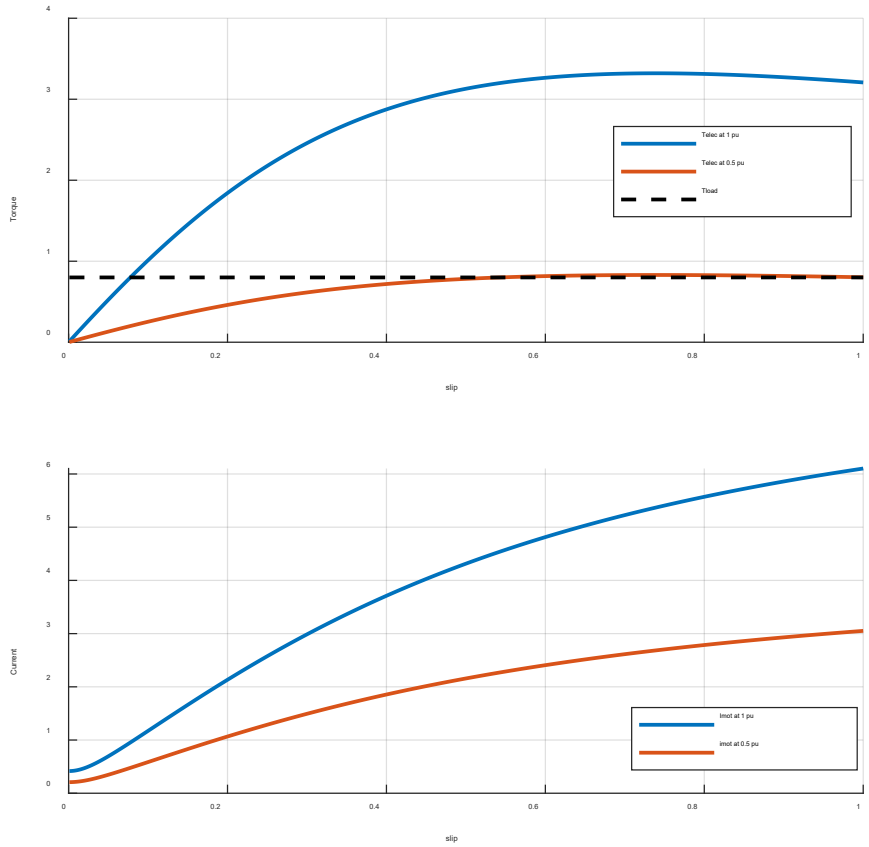

Figure 3-2
Torque – slip and current – slip characteristics of a NEMA type D motor

Table 3-2
Motor A parameters for commercial constant torque loads

Motor A (induction motor) parameters (NERC recommended for *commercial* type motors)							
LF	***Ra***	***Ls***	***Lps***	***Lpps***	***Tpo***	***Tppo***	***H***
0.75	0.02	1.8	0.12	0.104	0.08	0.0021	0.1

Table 3-3
Motor A parameters for industrial constant torque loads

Motor A (induction motor) parameters (NERC recommended for *industrial* type motors)							
LF	***Ra***	***Ls***	***Lps***	***Lpps***	***Tpo***	***Tppo***	***H***
0.8	0.01	3.1	0.1384	0.121	0.1028	0.0028	0.15

Protection model in motor A

All 3-phase motor models including motor A has the provision of capturing the aggregated response of the manufacturer installed protection that all customer equipment have. Typically, most motors have some form of under/over-voltage and/or over-current relays, and contactors.

The effect of the protection system is to trip a portion of the load as the system voltage drops and then reconnect a portion of the load as the voltage recovers over a preset threshold. In the composite load model, for 3 phase motors the aggregated response is captured by a staggered two stage tripping and reconnection. Table 3-4 lists a sample set of protection parameters for motor A. The parameters listed in Table 3-4 are subject to changes as more information on industrial motors and grid events are available. The readers are advised to check with the NERC/WECC LMTF for guidance on the most updated list of protection parameters.

The operation of the protection function is as follows:

1. if the voltage drops below Vtr1 for Ttr1 seconds, fraction Ftr1 of motor A trips,
2. if the voltage drops below Vtr2 for Ttr2 seconds fraction Ftr2 of motor A trips,
3. when the voltage recovers above Vrc1 for Trc1 seconds fraction Ftr1 of motor A reconnects, and
4. when the voltage recovers above Vrc2 for Trc2 seconds fraction Ftr2 of motor A reconnects.

Table 3-4
Motor A protection parameters for commercial and industrial type motors

	Vtr1	*Ttr1*	*Ftr1*	*Vrc1*	*Trc1*	*Vtr2*	*Ttr2*	*Ftr2*	*Vrc2*	*Trc2*
Commercial	0.5	0.03	0.5	0.8	0.1	0.6	0.15	0.25	1	9999
Industrial	0.7	0.05	0.3	1	9999	0.6	0.02	0.7	1	9999

Reference [7] presents a survey of trip and reconnection settings of a wide variety of 3 phase motors used by commercial class customers.

The Motor B Component

Motor B is used to represent an aggregation of 3-phase induction motors that drive high inertia variable torque loads. Typical loads that fall under this category are:

1. Large fans, and
2. Centrifugal compressors

Most commonly motor B is used to model large fans that are used in commercial/industrial blowers and air handlers and centrifugal compressors typically used in commercial/industrial grade large central cooling systems. Large fans and commercial centrifugal compressors to their design and dimensions typically have relatively higher inertia.

Motors that run variable torque loads typically have a standard NEMA type B design, which have medium starting torque capabilities and small operating slip around 0.5 - 5% (better power factor). Figure 3-3 shows the torque – slip and the current – slip characteristics of motor B motor at 1 pu and 0.55 pu terminal voltage. Observing the load torque and the electric torque characteristics in Figure 3-3 it can be inferred that motor B can be theoretically reaccelerated to a steady operating condition (for the shown load torque) at a stiff terminal voltage of 0.55 pu.

The values listed in Table 3-5 are the NERC recommended values when motor B is used to model an aggregation of commercial high inertia variable torque loads. Table 3-6 lists the NERC recommended parameters when motor B is used to model an aggregation of industrial high

inertia variable torque loads. Based on industry experience, an inertia constant (H) of 0.5s is recommended for modeling these loads. This inertia constant in reflected in the motor A parameters listed in Table 3-5 and Table 3-6.

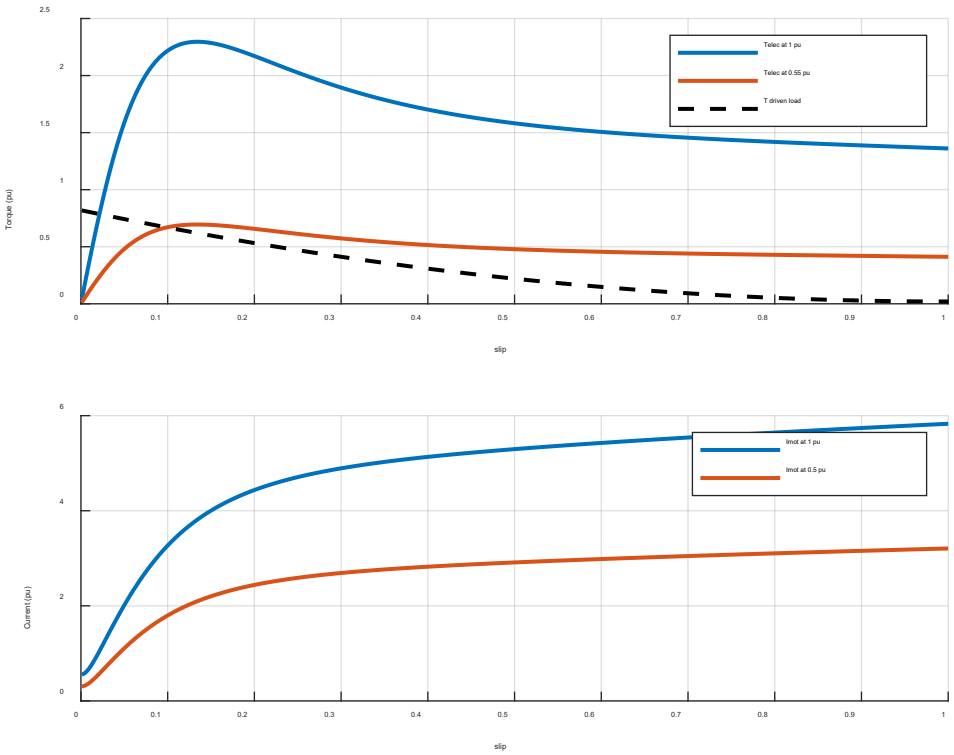

Figure 3-3
Torque – slip and current – slip characteristics of a NEMA type B motor

Table 3-5
Motor B parameters for commercial high inertia variable torque loads (fans etc.)

Motor B (induction motor) parameters (NERC recommended for *commercial* type motors)							
LF	***Ra***	***Ls***	***Lps***	***Lpps***	***Tpo***	***Tppo***	***H***
0.75	0.02	1.8	0.19	0.14	0.2	0.0026	0.5

Table 3-6
Motor B parameters for industrial high inertia variable torque loads (fans etc.)

Motor B (induction motor) parameters (NERC recommended for *industrial* type motors)							
LF	***Ra***	***Ls***	***Lps***	***Lpps***	***Tpo***	***Tppo***	***H***
0.8	0.01	4	0.1964	0.1639	0.893	0.0044	0.8

Protection model in motor B

The protection model of motor B is similar to the one in motor A. Table 3-7 lists a sample set of protection parameters for motor B in the composite load model. The parameters listed in Table 3-7 are subject to changes as more information on industrial motors and grid events are available. The readers are advised to check with the NERC/WECC LMTF for guidance on the most updated list of protection parameters.

Table 3-7
Motor B protection parameters for commercial and industrial type motors

	Vtr1	*Ttr1*	*Ftr1*	*Vrc1*	*Trc1*	*Vtr2*	*Ttr2*	*Ftr2*	*Vrc2*	*Trc2*
Commercial	0	9999	0	1	9999	0	9999	0	1	9999
Industrial	0.7	0.05	0.3	1	9999	0.6	0.02	0.5	0.75	0.25

The Motor C Component

The motor C component is used to model low inertia variable torque loads in the system. Typical low inertia, variable torque loads are the centrifugal pumps that are used widely for a variety of applications is circulation systems. Pump type loads have similar torque-speed dependence like fans, and hence NEMA type B design motors are typically used to drive these loads. Therefore motor C, like motor B have the same electrical parameters listed in Table 3-5 and Table 3-6 and the same torque-slip characteristics as shown in Figure 3-3. Centrifugal pumps have a small impeller diameter and therefore a significantly smaller inertia as compared to similar sized fans and compressors. To reflect the smaller inertia, an inertia constant of 0.1s is used for motor C. The parameter sets of Table 3-5 and Table 3-6 are repeated in Table 3-8 and Table 3-9 for the convenience of the readers.

Table 3-8
Motor C parameters for commercial high inertia variable torque loads (fans etc.)

Motor C (induction motor) parameters (NERC recommended for *commercial* type motors)							
Ls	***Lp***	***Lpp***	***Ll***	***Ra***	***Tpo***	***Tppo***	***H***
0.75	0.02	1.8	0.19	0.14	0.2	0.0026	0.1

Table 3-9
Motor C parameters for industrial high inertia variable torque loads (fans etc.)

Motor C (induction motor) parameters (NERC recommended for *industrial* type motors)							
Ls	***Lp***	***Lpp***	***Ll***	***Ra***	***Tpo***	***Tppo***	***H***
0.8	0.01	3.1	0.1954	0.1557	0.4759	0.0036	0.8

Protection models in motor C

The protection model of motor C is similar to the ones in motor A and motor B. Table 3-10 lists a sample set of protection parameters for motor C in the composite load model. The parameters listed in Table 3-10 are subject to changes as more information on industrial motors and grid events are available. The readers are advised to check with the NERC/WECC LMTF for guidance on the most updated list of protection parameters.

Table 3-10
Motor C protection parameters for commercial and industrial type motors

	Vtr1	*Ttr1*	*Ftr1*	*Vrc1*	*Trc1*	*Vtr2*	*Ttr2*	*Ftr2*	*Vrc2*	*Trc2*
Commercial	0	9999	0	1	9999	0	9999	0	1	9999
Industrial	0.7	0.05	0.3	1	9999	0.6	0.02	0.5	0.75	0.25

The Motor D Component

The motor D component of the composite load model is used to represent the aggregated response of single-phase residential air-conditioners and heat ventilation and air-conditioning (HVAC) systems connected downstream of a distribution substation. Residential air-conditioners typically have a positive displacement compressor, which is either a reciprocating type (piston armed) or scroll type. The motor-compressor set for a residential HVAC unit has a very small inertia and therefore prone to stalling during voltage sags [8]. Stalled single phase induction motors have a significantly higher active and reactive power consumption, and hence a large number of stalled residential HVAC systems typically cause a slow voltage recovery following a fault. This phenomenon is called fault induced delayed voltage recovery or FIDVR [8].

The motor D model is a performance-based model that captures the changes in the active and reactive power consumption of the motor using algebraic equations. Figure 3-4 shows the schematic diagram of the motor D model along with the associated protection models.

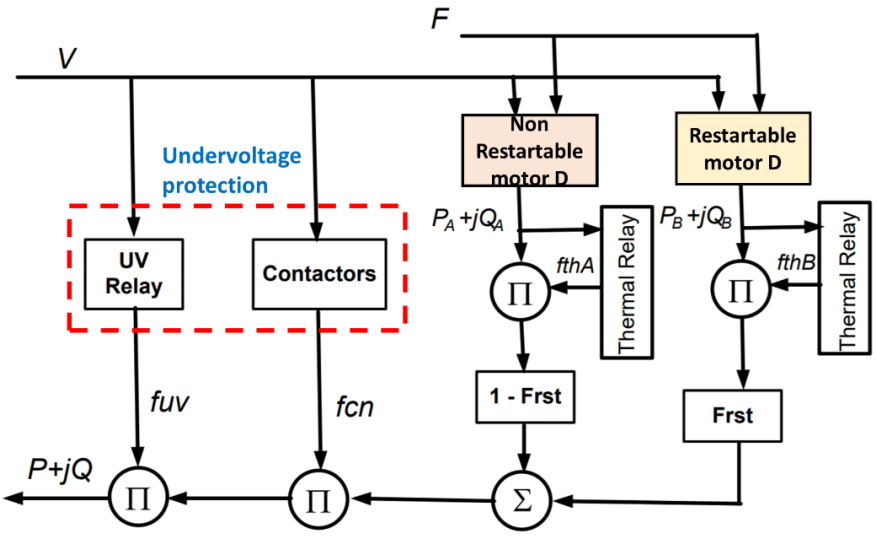

Figure 3-4
Schematic of the motor D model [9]

The active and reactive power characteristics of the model were developed based on extensive testing of numerous residential HVAC systems in laboratory facilities. The active and reactive power consumption of motor D is shown in Figure 3-5. The active and reactive power characteristics of motor D (Figure 3-5) has three distinct regions:

a. run state I,
b. run state II, and

c. stall state.

The initial values of active and reactive power (P_0 and Q_0) for the motor D model are calculated during the initialization process. The voltage level *Vstallbrk* in Figure 3-5, where the run state curve intersects the stall state curve is also computed automatically during model initialization [1, 2, 3].

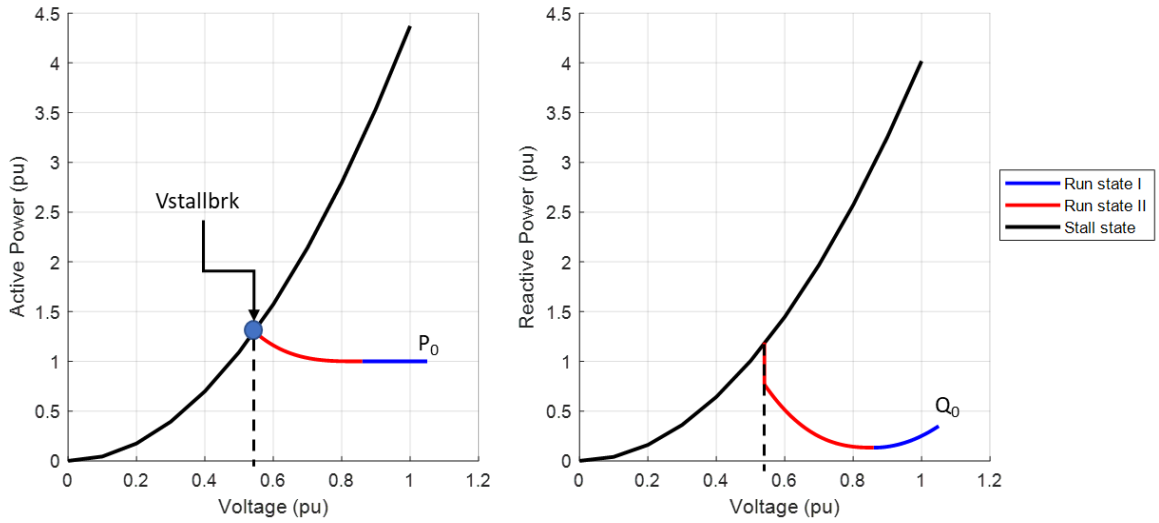

Figure 3-5
Active and reactive power consumption of the motor D component

Each of the different states in Figure 3-5 are represented by separate algebraic equations. The detailed equations for the motor D model can be found in Appendix A. The NERC recommended default parameters used for the motor D model is listed in Table 3-11. Note that the parameters listed in Table 3-11 are the best estimates available during the compilation of this work. The readers are advised to check with the NERC/WECC LMTF for the most updated parameter set while using the model. The detailed description of the parameters can be found in the user manuals of the various software vendors [1-4] and are used in the equations listed in Appendix A.

Table 3-11
NERC recommended default parameter set for motor D

Parameter	Value	Parameter	Value
LFm	1	**Tth**	15
CompPF	0.98	**Th1t**	0.7
Vstall	0.45	**Th2t**	1.9
Rstall	0.1	**Tv**	0.025
Xstall	0.1	**Tf**	0.05
Tstall	0.03	**LFadj**	0
Frst	0.2	**Kp1**	0
Vrst	0.95	**Np1**	1
Trst	0.3	**Kq1**	6
Fuvr	0.1	**Nq1**	2
vtr1	0.6	**Kp2**	12
ttr1	0.02	**Np2**	3.2
vtr2	0	**Kq2**	11
ttr2	9999	**Nq2**	2.5
Vc1off	0.5	**Vbrk**	0.86
Vc2off	0.4	**CmpKpf**	1
VC1on	0.6	**CmpKqf**	-3.3
VC2on	0.5		

Since the motor D model is a performance model, the transition of the model from the running state to the stall state and vice versa is determined by user specified voltage and time thresholds. These thresholds are set by the *Vstall*, *Tstall* pair, and *Vrst*, *Trst* pair respectively as listed in Table 3-11. The transition of the model between the different states is explained as follows:

a. **Transition from run state to the stall state**: when the voltage at the composite load model terminal dips below the user specified *Vstall* for a time duration of *Tstall*, the motor transitions to the stall condition.

b. **Transition from stall state to the run state**: When the voltage at the terminal of the composite load model where motor D has stalled recovers over *Vrst* for a time duration of ***Trst,*** the restartable portion of the composite load model (given by Frst in Table 3-11 and Figure 3-4) transitions back to the run state. Note that the non-restartable portion the motor D remains stalled state for the remainder of the simulation once it has stalled.

Depending of the values of the *Vstall* and *Tstall*, the transition of motor D from a run to a stall condition can vary notably. This transition has been explained for some sample values of *Vstall* and *Tstall* in the following sub sections.

Vstall = any value, Tstall = 999 (Stalling disabled)

When *Tstall* is set to 999 in a simulation, it is expected that the residential HVACs modeled in the system do not go into a stalled condition where they draw excessive active and reactive power. The variation of the active and reactive power drawn by motor D as the terminal voltage

varies, is shown in Figure 3-6 by the blue arrows. As seen in Figure 3-6 the active and reactive power consumption of motor D does not increase excessively from its steady state values even when the terminal voltage dips to low levels.

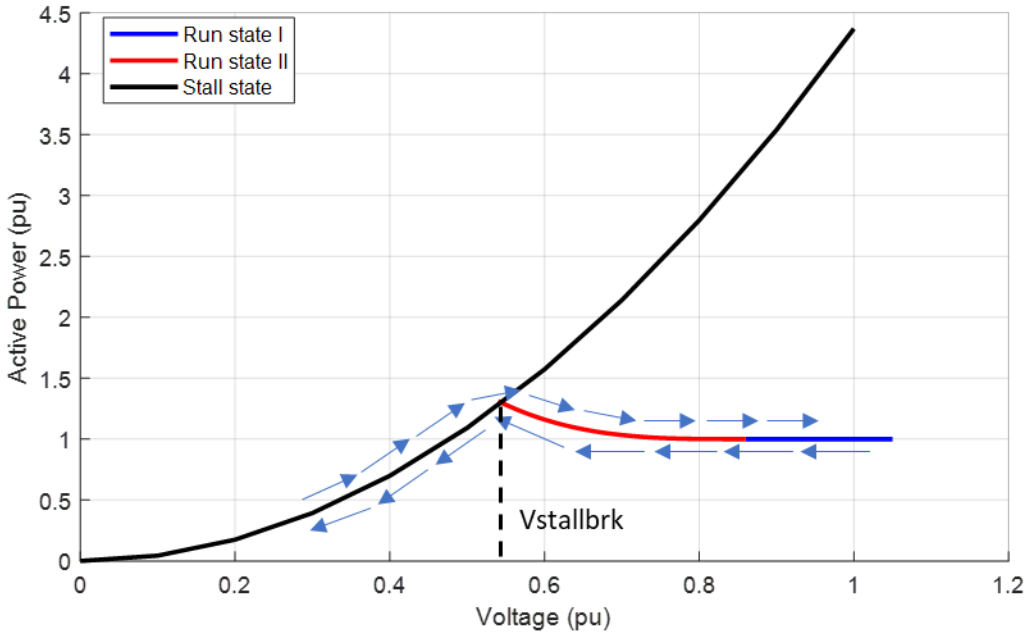

Figure 3-6
Motor D active power change with voltage when stalling is disabled (Tstall = 9999)

Vstall <Vstallbrk, Tstall = 2 – 3 cycles (60 Hz) (Stalling enabled)

When stalling is enabled, the value of *Tstall* is set close to 2-3 cycles and the value of *Vstall* can be either greater or less than the *Vstallbrk* point shown in Figure 3-7. When *Vstall* is set lower than *Vstallbrk*, the transition of motor D from a run condition to a stall condition is smooth as indicated by the blue arrows in Figure 3-7. In this case, the active and reactive power drawn by motor D increases significantly as the terminal voltage recovers (as shown by the arrows). This represents a widespread stalling of residential HVACs in a distribution system due to a voltage sag in the system.

As the voltage recovers above *Vrst* for time *Trst*, the restartable fraction (*Frst*) of motor D transitions to the run state whereas the remaining fraction (1-Frst) continues to remain stalled. This is shown by the purple and brown arrows in Figure 3-7 respectively.

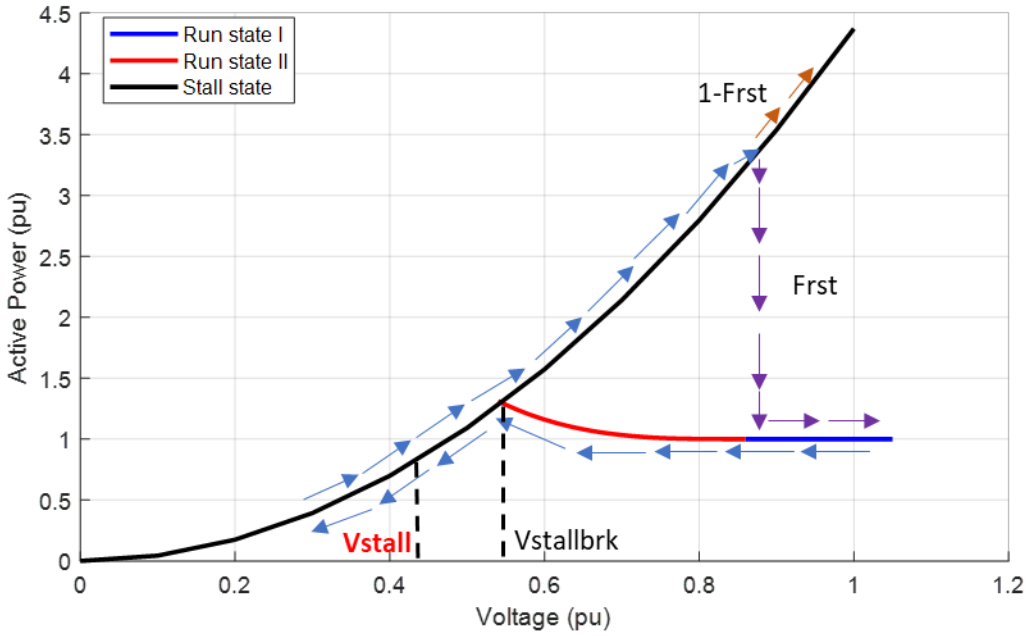

Figure 3-7
Motor D active power change with voltage when stalling is enabled and Vstall < Vstallbrk (Tstall = 2-3 cycles)

Vstall >Vstallbrk, Tstall = 2 – 3 cycles (60 Hz) (Stalling enabled)

If *Vstall* is set higher than the value *Vstallbrk*, motor D exhibits an abrupt jump in the active and reactive power consumption as the motor transitions into a stall state from the run state. This is shown by the blue arrows in Figure 3-8. The remainder of the behavior is similar to that described in the previous section.

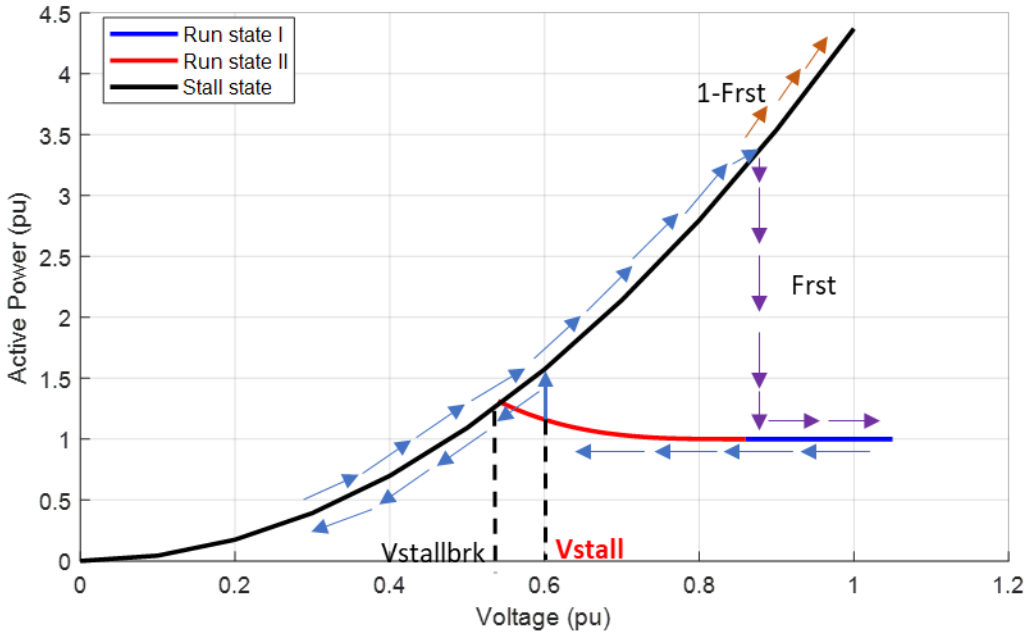

Figure 3-8
Motor D active power change with voltage when stalling is enabled and Vstall > Vstallbrk (Tstall = 2-3 cycles)

Protection models in motor D

The motor D component allows for modeling the aggregated effect of three different protection features that covers the spectrum of protection options typically found in residential HVAC systems. The three protection features are:

1. the thermal (overcurrent) protection of the compressor motor,
2. contactor based instantaneous undervoltage protection
3. time dependent undervoltage protection

Table 3-1 lists the parameters in the motor D model related to these protection features and their default values.

Table 3-12
NERC recommended default protection parameter set for motor D

Parameter	Value
Fuvr	0
vtr1	0
ttr1	9999
vtr2	0
ttr2	9999
Vc1off	0.5
Vc2off	0.4
VC1on	0.6
VC2on	0.5
Tth	15
Th1t	0.7
Th2t	1.9

A detailed description of each protection function is as follows:

1. **Thermal relay:** All residential HVAC compressors are equipped with thermal overcurrent protection which trips the HVAC compressor when the current drawn by the units exceeds its locked rotor ampere rating for a certain period. This protection typically takes the form of a bimetallic plate that forms the contact for the motor. When the motor draws excessive current for a significant period of time, the heating of the motor windings and bimetallic plate results in the contact being opened and thus the motor tripping. It then requires many minutes to cool down before the motor contact is established and it can be restarted. To model this physical phenomenon an emulation of this process is made with what is referred to here as a thermal relay. The model computes the $I^2Rstall$ losses (essentially heating energy in the conductors) and uses a time constant Tth to compute a value which serves as a proxy for the compressor motor winding temperature. This is shown in Figure 3-9. As the temperature increases beyond Tth1 the motor D load is linearly tripped with the entire fraction tripped as the temperature rises beyond Tth2. **Note:** this linear tripping (rather than a sudden trip) is done to emulate the fact that since this is an aggregate load model, not every single compressor motor will trip at the same instant. Thus, again it is an emulation of the expected staggered tripping of the individual (100's) of motors that are being modeled by a single aggregated Motor D model.

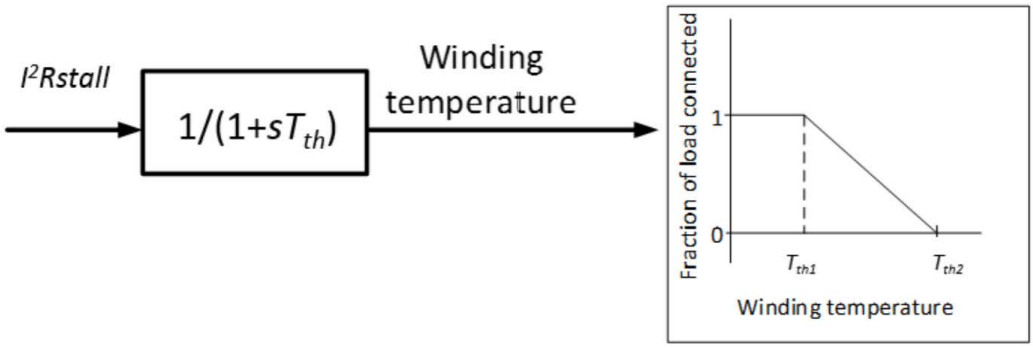

Figure 3-9
Motor D thermal relay model

2. **Contactor model**: The contactor model represents a linear trip of the motor D component as the voltage dropped below the threshold *Vc1off* and trips the motor D component entirely when the voltage reaches *Vc2off*. Similar to the tripping process, the contactor linearly reconnects the motor D component as the voltage starts to recover above *Vc2on* and reconnects the entire motor D component after the voltage recovers above *Vc1on*. The contactor operation is shown in Figure 3-10. The black arrows in Figure 3-10shows the contactor operation as the voltage dips and then recovers from an intermediate voltage level (between *Vc1off* and *Vc2off*). Note that the contactor model does not have a time comparator and hence trips/reconnects the motor D fraction almost instantaneously as the voltage thresholds are breached. This implementation is in line with the observations made for actual contactor operation during lab testing of residential HVACs.

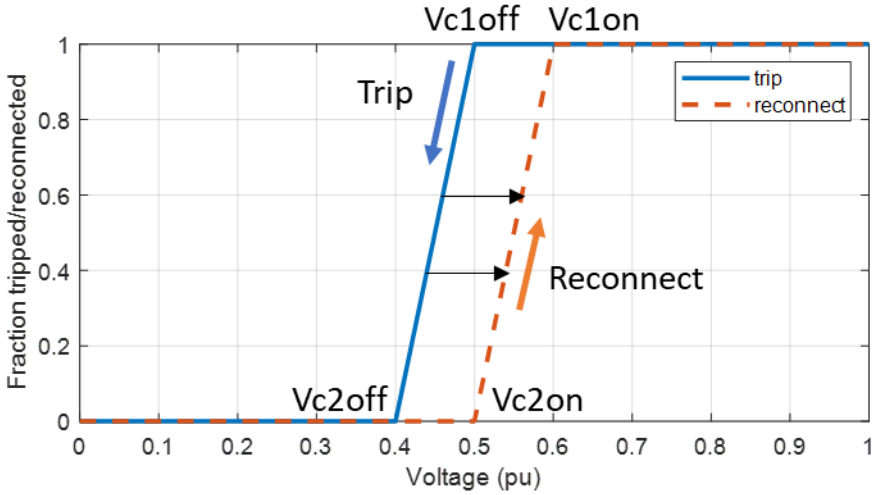

Figure 3-10
Motor D contactor characteristics

3. **Undervoltage relay:** In addition to the contactor model, a time dependent undervoltage trip relay is also available in the motor D model. If the terminal voltage at the composite load model drops below *Vtr1* for *Ttr1* seconds ***or*** if the voltage drops below *Vtr2* for *Ttr2* seconds

the fraction *Fuvr* is **permanently** tripped for the remainder of the simulation. This protection is used to represent the tripping of some residential HVACs which take a significantly longer time (1 minute – 5 minutes) to reconnect once tripped. Such protection schemes are often used in residential HVACs to protect the compressor from cycling (a cycle of failed restarts) and reverse rotation after momentary sags.

The Power Electronic Component

The power electronic component of the composite load model is intended to model all consumer loads that are connected to the system through an inverter-based interface. These types of loads include consumer electronic devices like computers, televisions etc. to variable speed drive interfaced motor loads. The power electronic component has a simple algebraic representation with:

1. a constant active and reactive power consumption over a user specified voltage range, and
2. a linear reduction in the active and reactive power consumption as the voltage drops below the user specified voltage range, to represent the undervoltage trip of these devices.

The model also allows for a user specified percentage of electronic load to reconnect back to the system as the voltage recovers above the trip threshold. The electronic load behavior is shown in Figure 3-11. The model starts tripping load when the terminal voltage drops below *Vd1* and drops 100% of the load below *Vd2*. The model keeps a track of the minimum terminal voltage *Vmin* and uses it along with the parameter *frcel* to compute the fraction of load reconnected as the voltage recovers.

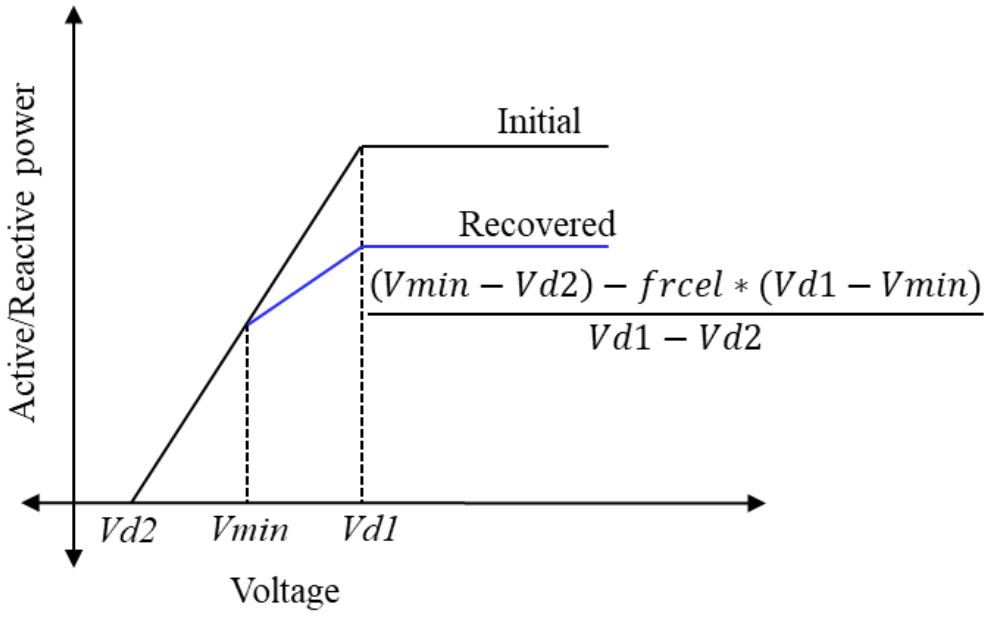

Figure 3-11
Power electronic component of the composite load model

The Static Load Component

The static load component is used to represent the constant impedance (Z), constant current (I) and constant power (P) loads in the system. The ZIP component is typically used to model resistive heating type loads (heating, cooking etc.), and incandescent and LED type lighting loads in the system. The detailed equations of the ZIP model are provided in Appendix A.

A Note on Motor Stalling

Stalling of motors following a voltage disturbance is a topic of great interest for power system planners. Stalling of a motor is a condition when a motor runs down to a zero speed and then gets stuck in a locked rotor condition, unable to restart. Motors typically stall when the terminal voltage drops significantly during a voltage disturbance. If the motor is unable to restart and remains in a stalled (locked rotor) it acts as a constant impedance load, drawing a high amount of both active and reactive power. In this stalled (high slip) condition, the reactive power drawn by the motor is significantly higher than its active power consumption. This can be observed in Figure 3-5 for a single-phase induction motor. A three-phase induction motor has a similar behavior as well.

The stalling of an induction motor (single and three-phase) depends on a number of factors, which include:

1. The severity of the disturbance
2. The design of the induction motor
3. The nature of the driven load.

A detailed analysis of stalling of induction motors is beyond the scope of this document, however a brief discussion on this topic is presented here.

During a momentary voltage sag (caused by a fault) a motor starts to decelerate. Once the voltage recovers, if the motor cannot generate enough torque to reaccelerate back the motor decelerates and goes into a stalled condition. The ability of a motor to generate reaccelerating torque depends on

1. *The speed to which a motor has decelerated during a disturbance*: In general motors that drive high inertia loads have a slower rate of deceleration as compared motors that drive low inertia loads. Motors that decelerate less are more likely to be able to reaccelerate.
2. *The driven load behavior*: Loads like fans and centrifugal produce a torque that decreases as the speed decreases. It may be easier for a motor to generate enough torque at a lower speed to overcome this load torque and reaccelerate. On the other hand, a motor driving a constant torque load like a positive displacement pump or a compressor may not be able to produce enough reaccelerating torque and remain in a stalled condition.
3. *The design of the motor*: The design of the motor plays an important role in its ability to reaccelerate back. Some special design three phase motors like NEMA type D motors produce very high torque under a low slip condition. These motors can reaccelerate against significantly high torque. The torque producing capability of a three-phase induction motor depends on this rotor resistances and reactances and whether they have a single cage or a

double cage or deep bar design. In the case of a single-phase motor, this also depends on whether the motor has a properly designed starting capacitor.

It is worthwhile to mention that a combination of the three factors listed above is responsible for causing a motor to stall. It is possible that a motor with a poor design may stall even if the driven load has a high inertia and may have a variable torque characteristic. Similarly, a motor driving a constant torque load with low inertia may not stall if the motor is designed well to produce the required reaccelerating torque.

In practice, the single-phase motors driving residential HVAC systems are the motors that are most likely to stall. This is due to the fact that single phase motors have considerably lower inertia as compared to three-phase induction motors. Moreover, even if three phase motors stall it happens over a period of seconds, whereas single phase motors due to their low inertia can stall within a few cycles. Additionally, many large motors used in industrial as well as commercial applications have protection systems in place that trips these motors when a voltage dip is detected. This is done to protect the motor against damage from high currents. As such these motors are not likely to remain stalled on the power system and draw large amounts of current.

Finally, the three-phase motors modeled in the composite load have a full representation of the flux as well as the electromechanical dynamics. Therefore, if the motor parameters are chosen in a particular way and the terminal voltage remains significantly depressed, the motor A, B and C components can all go into a stalled condition like the motor D. An example of a study where stalling of three phase motors were observed can be found in [10]. A detailed treatment on stalling of motors can be found in [12], [13].

References

[1] PSS®E 33.9 Documentation

[2] PSLF 19.02 User's Manual

[3] Powerworld documentation, available at: http://www.powerworld.com/WebHelp/Default.htm.

[4] TSAT 16.0 User Manual

[5] *Technical update on load modeling:* EPRI, Palo Alto, CA: 2017, 3002010754.

[6] WECC composite load model benchmarking summary, available online: https://www.wecc.org/Administrative/Composite%20Load%20Model%20Bench%20Marking%20Summary%20Report%20v5.pdf

[7] PNNL report 24468*, Commercial building motor protection response report*, available online: https://www.pnnl.gov/main/publications/external/technical_reports/PNNL-24468.pdf

[8] NERC report, *A technical reference paper fault induced delayed voltage recovery,* available online: https://www.nerc.com/docs/pc/tis/FIDVR_Tech_Ref%20V1-2_PC_Approved.pdf

[9] WECC composite load model specifications, available online: http://home.engineering.iastate.edu/~jdm/ee554/WECC%20Composite%20Load%20Model%20Specifications%2001-27-2015.pdf

[10] P. Pourbeik, R. J. Koessler and B. Ray, "Addressing Voltage Stability Related Reliability Challenges of San Francisco Bay Area with a Comprehensive Reactive Analysis", *Proceedings of IEEE PES* General Meeting, July 2003.

[11] C. Taylor, *Power System Voltage Stability*, McGraw-Hill, 1994.

[12] J. H. Dymond, "Stall time, acceleration time, frequency of starting: the myths and the facts (electric motors)", *IEEE Trans. Industry Applications,* January 1993.

4
PARAMETERIZING THE COMPOSITE LOAD MODEL

Developing a model to provide a better representation of the load is only halfway towards having an appropriate representation of the load in dynamic studies. Another important aspect of load modeling is parameterizing the load model such that the model is reasonably representative of the aggregated load response. Parameterizing a load model is a challenging task since the system load is always changing in its level and composition, and the fact that most transmission planners have poor visibility into the very details of the consumer loads. To tackle the challenge of load model parameterization, two different approaches have been used in tandem, and the combined use of these approaches have shown promising results for model parameterization. The two commonly used and complementary approaches are:

1. The component-based aggregated load modeling approach [1],
2. The measurement-based aggregated load modeling approach [2 - 4].

A brief description of these two approaches and the common tools that implement these approaches are described in the following sections. It is worthwhile to emphasize that modeling and parameterizing a single load component like a motor or an industrial drive is a much simpler process, that modeling an aggregation of such devices that are operating in a distribution feeder. To model and parameterize a single device, the approach is to develop a model based on first principles and then parameterize the model based on some staged test on the actual equipment. However, for aggregated load modeling, this approach is challenging since:

1. The aggregation of loads is intended to model a mix of devices from different manufactures that are distributed downstream of an aggregation point in a random manner.
2. Stage testing of an aggregation of devices is not possible and grid events that might provide measurements to validate and parameterize these models are quite rare. This point will be elaborated later.

The Component-Based Load Modeling Approach

The component-based load modeling approach is a bottoms-up approach where the end-use consumer load types are first identified using a survey type approach and then the end use types are assigned to the different components of the composite load model through some rules of association. This process differs slightly for commercial and residential loads as compared to that for industrial loads. It is important to emphasize that the component-based load modeling approach is used to determine only the fractions of the different components, *Fma, Fmb, Fmc, Fmd* and *Fel* parameters of the composite load model. The physical parameters of the models like the resistances and reactances of the induction motors cannot be derived using this method. A measurement-based approach is more suitable for estimating those components.

The component-based load modeling process starts with determining the load classes at a distribution substation. For the purposes of load modeling, the load class at a substation is determined by the percentage composition (in MW preferably) of:

a. Residential loads e.g. single and multi-family homes, condominiums, apartments etc.

b. Commercial loads e.g. grocery store, strip malls, hotels and motels, office buildings etc.

c. Agricultural loads e.g. Farms

d. Industrial loads.

As an example, a residential class feeder may comprise of about 70% – 90% pure residential loads like houses and apartments, and 10%-30% commercial loads like grocery stores and supermarkets. Similarly, an example of a typical commercial feeder can be a downtown area, where 80% to 100% of the loads comprise of power consumption in commercial offices, and hotels. Certain feeders in suburban areas can also have a mix of residential houses along with farms which are agricultural loads. These feeders are typically called rural agricultural feeders.

It is important to highlight that the percentages of the individual components at a load serving substation will typically vary throughout the day. The load class should therefore be estimated separately at load buses for peak and off-peak hours, which are typically of interest for transmission planners. In general, as the industry transitions towards multi-hour analysis, the load class should be estimated for each of the pertinent hours for which the system is being analyzed.

Once the load class at each distribution substation is determined, the next task in the component-based approach is to determine the proportion of end use load components of the residential commercial, agricultural and industrial load classes. Once the end uses are determined appropriately, a set of rules of association is used to determine the final percentages of the motor A, B, C, D, the power electronic component and the static (ZIP) load components. The block diagram of the process is shown in Figure 4-1. The process of determining of end use load composition for residential, commercial, agricultural and industrial loads and finally deriving the composite load model percentages is detailed in the following subsections.

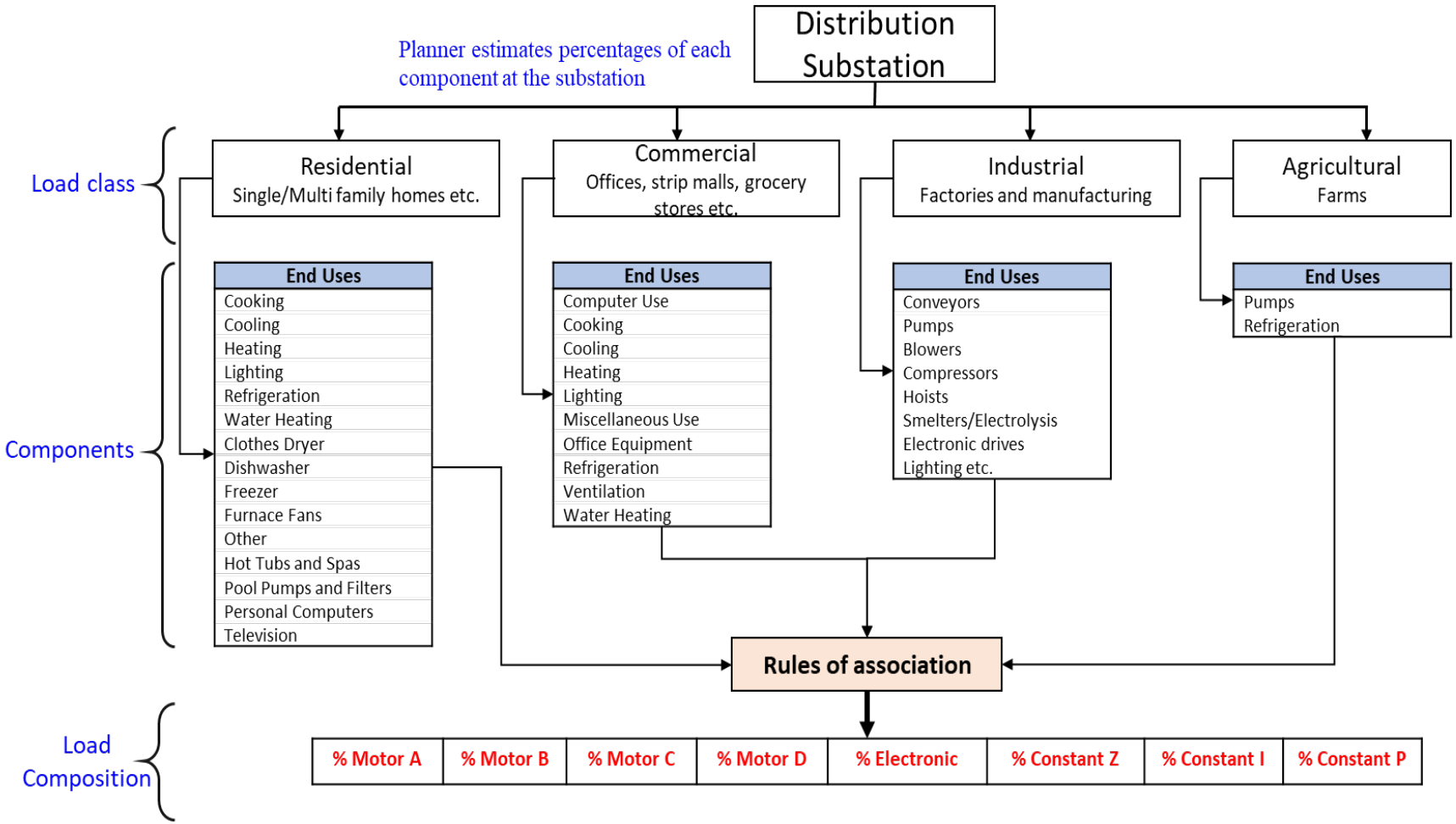

Figure 4-1
Component based load modeling approach

Residential and Commercial Load Composition Estimation

A description of the component-based approach to load composition estimation for residential and commercial loads are presented here. Various tools like the EPRI Load Composition Export Tool (LCET) [5], the NERC/DOE Load Model Data Tool (LMDT) and the Pacific Northwest National Lab's Load Model Data Tool [6] have automated this approach and are being used by different utilities in the United States and elsewhere. Although different tools approach this problem in a slightly different way, the basic concept and steps remain the same. The core steps involved in a component-based load modeling approach are as follows:

1. A load model of an individual consumer load block e.g. residential house or a commercial building is first developed. This load model includes hourly (typical) electrical load shapes for consumer end use equipment like heating, cooling, cooking, lighting, consumer electronics etc. Figure 4-2 shows some example normalized load shapes for a residential and a commercial building.
2. A statistical or a typical mix of the individual load blocks that comprise the aggregated load at a location is then determined using census data or in consultation with the distribution companies in the utility's footprint. The load aggregation point is typically at the low side of a distribution substation transformer.
3. The load shapes developed in step one for each individual load block is then added based on the statistical mix derived in step 2 form an aggregated load shape at a load aggregation point.
4. Finally, a set of rules of association are used to then convert this aggregated hourly load shapes into hourly composite load model records, and the user can then choose a desired composition of the different components based on the hour under study (typically peak and off peak). Note that the load shapes vary depending on the season, since certain loads like air-conditioning and heating loads are ambient temperature dependent. Therefore, different load shapes are used for selecting peak and off peak hours for different seasons. Some sample rules of association used to map the residential and commercial end use load types for the composite load components are listed in Table 4-1 and Table 4-2. Again, the readers are strongly encouraged to consult the manuals of any tool that they are using for the exact rules of association being used. These may differ slightly or be the same between the different tools. Appendix A lists the rules of association that are used in the EPRI LCET and the NERC LMDT tools.

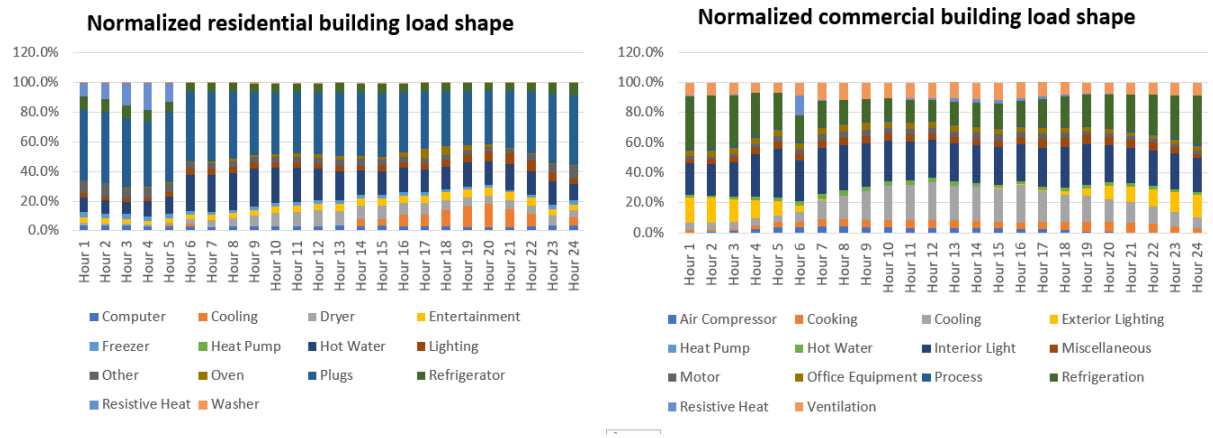

Figure 4-2
Example of normalized load shapes for a residential and a commercial building.

Table 4-1
Example rules of association for residential end use types (Single and Multi-family homes)

End Use	Motor A	Motor B	Motor C	Motor D	Pelec	z	i	p
Computer Use	0	0	0	0	1	0	0	0
Cooking	0	0	0	0	0	1	0	0
Cooling	0.65	0.05	0.1	0	0.2	0	0	0
Heating	0	0	0	0	0	1	0	0
Lighting	0	0	0	0	0	0	1	0
Miscellaneous Use	0	0	0	0	0.5	0.5	0	0
Office Equipment	0	0	0	0	1	0	0	0
Refrigeration	0.8	0.1	0.1	0	0	0	0	0
Ventilation	0	0.7	0	0	0.3	0	0	0
Water Heating	0	0	0	0	0	1	0	0

Table 4-2
Example rules of association for commercial end use types (grocery stores and strip malls)

End Use	Motor A	Motor B	Motor C	Motor D	Pelec	z	i	p
Cooking	0	0	0	0	0	1	0	0
Cooling	0	0.1	0.1	0.8	0	0	0	0
Heating	0	0	0	0.1	0	0.9	0	0
Lighting	0	0	0	0	0	1	0	0
Refrigeration	0	0	0	1	0	0	0	0
Water Heating	0	0	0	0	0	1	0	0
Clothes Dryer	0	0	0.4	0	0	0.6	0	0
Dishwasher	0	0.5	0	0	0	0.5	0	0
Freezer	0	0	0	1	0	0	0	0
Furnace Fans	0	1	0	0	0	0	0	0
Other	0	0	0	0	0.5	0.5	0	0
Hot Tubs and Spas	0	0	1	0	0	0	0	0
Pool Pumps and Filters	0	0	1	0	0	0	0	0
Personal Computers	0	0	0	0	1	0	0	0
Television	0	0	0	0	1	0	0	0

Within the United States, various open access resources and databases are available to aid the component-based load composition estimation for residential and commercial loads. A list of these some of these resources are as follows:

1. The US DOE's residential energy consumption survey (RECS) [7], the BPA residential building stock assessment (RBSA) [8] provides information on the residential end use load shapes.
2. The US DOE's commercial building energy consumption survey (CBECS) [9] and California end use load shapes (CEUS) database [10].
3. The United States census division data [11], and finally
4. The typical meteorological data sets (TMY3) [12] and National oceanic and atmospheric administration (NOAA) [13] weather data. The weather data is required for determining the temperature and humidity sensitive loads like cooling and space heating, which comprise a significant chunk of the residential and commercial loads.

Note that the tools developed for creating the load model fractions use these databases and transmission planners are typically not required to deal with these databases directly.

Agricultural Load Composition Estimation

The bulk of the agricultural load typically consists of small and large pumps that are required for irrigation and some cooling load required for storing produce. A typical load composition of agricultural load is shown in Table 4-3. In recent years, commercial vertical farming (also called indoor or container farms) are becoming more and more popular. These farming loads can have significantly higher proportions of lighting as well as HVAC load in addition to the pumps for irrigation.

Table 4-3
Load composition for agricultural load

Motor A	Motor B	Motor C	Motor D	Pelec	Z	I
0.15	0.2	0.2	0	0.2	0.1	0.15

Industrial Load Composition Estimation

The industrial load composition estimation process is slightly different from the residential and commercial load composition estimation process. Industrial loads typically do not vary as a function of weather like commercial and residential loads. In addition, similar industrial loads typically tend to have similar processes and hence the load components tend to be approximately similar. Therefore, from the perspective of transmission planning, a single type of load composition can be used to model a broad range of similar industrial plans. As an example, although different aluminum smelters may have different technologies, from the perspective of their impact on the bulk system all aluminum smelters can be represented by the same load composition. Therefore, if the typical processes in an industry is known based on some surveys, literature and experience, a set of rules of association can be used to derive the component estimates. Table 4-4 lists the NERC default industrial load composition for some industrial load types. It is worthwhile to mention that in most new industrial facilities the overwhelming majority of motor loads are connected through variable speed drives (VSDs). As such, a recommended practice would be to revisit the industrial load composition estimates regularly and update them to reflect such changes in technology adoption.

It should be noted that, these default compositions are not intended for performing specialized studies, where the industrial load may have a significant impact on the local system. In such cases, a detailed model of the processes needs to be developed for the industrial facility in order to perform such studies.

Table 4-4
NERC default load composition for some industrial load types

Industrial Load Type	PSLF Code	Motor A	Motor B	Motor C	Motor D	Pelec	Z	I
Petro-Chemical Plant	IND_PCH	0.1	0.4	0.3	0	0.15	0.02	0.03
Oil Pumping	IND_OIL	0.3	0	0.4	0	0.3	0	0
Shale Gas Extraction Plant	IND_SHG	0	0.2	0.4	0	0.4	0	0
Liquified Natural Gas	IND_LNG	0	0.3	0.2	0	0.5	0	0
Paper Mill, Kraft Process	IND_PMK	0.1	0.2	0.3	0	0.3	0.05	0.05
Paper Mill with Refiners	IND_PMT	0.05	0.6	0.15	0	0.15	0.02	0.03
Lumber Mill	IND_LMB	0.4	0.2	0.3	0	0	0.05	0.05
Mining	IND_MIN	0.25	0.25	0.3	0	0.2	0	0
Aluminum Smelter	IND_ASM	0.05	0	0.05	0	0.05	0.85	0
Steel Mill	IND_SML	0.15	0.35	0.25	0	0.15	0.05	0.05
Car Manufacturing	IND_CAR	0.15	0	0.3	0	0.3	0.1	0.15
Semiconductor	IND_SCD	0	0.25	0.3	0	0.4	0	0.05
Server Farm	IND_SRF	0	0	0.1	0	0.9	0	0
Industrial - Other	IND_OTH	0.1	0.3	0.3	0	0.2	0.05	0.05
Transportation - Rail	IND_RAIL	0	0	0.05	0	0.95	0	0
Power Plant Auxiliaries	PPA_AUX	0	0.4	0.3	0	0.2	0.05	0.05
Irrigation and pumping	AGR_IRR	0	0	1	0	0	0	0
Food processing	AGR_PRO	0.6	0	0.25	0	0.05	0.05	0.05

The Measurement-Based Load Modeling Approach

A measurement-based approach relies on developing a model structure based on an estimate of the underlying components and then using measurement data to parameterize the model structure. In the context of load modeling, a measurement-based approach would require a measurement of voltages, frequency and current, or voltages, frequency and power (active and reactive) for a grid event, that will then be utilized to parameterize the composite load model. The core steps involved in the measurement-based approach are as follows:

1. Derive raw measurements of voltage and current, or voltage and power (active and reactive) for a grid event.

2. Process the raw measurements such that it can be used in the relevant modeling framework (positive sequence, phasor or electromagnetic transient simulation platform).

3. Use a framework to play in the input voltage and frequency into the model and tune the model parameters to achieve a reasonable match between the measurements of active and reactive power and the model output.

Even though the process sounds straightforward, there are significant challenges with using a measurement-based approach. These challenges revolve around the acquisition of measurement data that is needed for the measurement-based approach. The main challenges are as follows:

1. **Availability of measurement devices**: For a measurement-based approach the measurement needs to be made closer to the load aggregation point. However, majority of measurement devices which can be used for load modeling like phasor measurement units (PMUs), micro PMUs, and digital fault recorders (DFRs) are typically placed at high voltage buses and generator buses. The measurements from these devices are influenced (or polluted) by dynamic response of other equipment in the power system and may not be directly usable for a measurement-based load modeling approach. In theory, for perfect measurement based modeling, the relevant measurements need to be made at the location or as close as possible to the location where the model will used in the simulation studies (i,e. at the high side of the distribution substation transformer). If load models connected to a 12.47 kV bus in simulation studies is parameterized based on measurements made at a 345 kV level transmission bus, using a least-squares minimization approach, it is highly likely that the optimization exercise would fail. In general, such an exercise is not recommended since any optimization method would parameterize (or try to parameterize) the load model to account for dynamic responses from other power system equipment that may be influencing the measurements at the transmission bus. Having said that, transmission level measurements sometimes do provide valuable information on load loss and voltage recovery rate in the system. In such cases, this information along with engineering judgement can be used to manually tune multiple instances of nearby load models to replicate the event. It is also worthwhile to mention that, load dynamics are a mix of electromagnetic and fast electromechanical transients which are significantly fast. As such, the entirety of the load dynamic response is not likely to be captured in PMU measurements because of the filtering of signals in PMUs. This important factor should be given due consideration when PMU measurements are used for load model as well as event validation.

2. **Availability of events**: Even though in recent years many utilities made significant investments for installing measurement devices like phasor measurement units (PMUs) and micro-PMUs closer to load serving substations, acquiring a relevant event can still be challenge. Typically, in transmission planning three phase faults are studied as these are the most severe type of faults on the transmission system. In addition to this, such events are studied during system peak conditions. Therefore, ideally it is expected that the load models used in the studies are parameterized based on measurements of three-phase faults made during system peak conditions (or heavy load conditions). Three-phase faults by nature are rare for most systems. In addition to that, having a three-phase fault coincident with the system peak conditions can be extremely rare. Since single phase faults are more common in power systems, measurement made for single phase faults are typically not sufficient to parameterize positive sequence models used in transmission planning studies. As an example, the response of a three-phase motor to an unbalanced fault cannot be captured adequately in positive sequence simulations. Therefore, parameterizing a positive sequence model of a 3-phase induction motor (motor A, B, and C) using the positive sequence component of the unbalanced 3 phase voltage and 3 phase power can result in an erroneous parameterization of the model. In addition, single line to ground faults are not known to cause widespread residential HVAC stalling that leads to FIDVR. As such, these fault

measurements are not sufficient to parameterize the motor D component of the composite load model. The only parameters of the composite load model that can be tuned using single-phase to ground fault recordings are the aggregate protection settings. An estimate of load lost during a single line to ground fault can be used to adjust the trip settings in the composite load model.

EPRI at present has a tool, the load model data processing and parameter derivation (LMDPPD) [13] tool that automates the process of measurement-based load modeling when relevant measurements are available.

Recommendations on Load Model Parameterization

It is important to highlight that both the approaches, the component-based and the measurement-based, are not mutually exclusive approaches. Ideally, both these approaches are needed for proper load model parameterization as these approaches complement each other.

Most measurement-based approaches require an optimization method that reduces the least squares error between the measurements and model output by modifying the control variables, in this case the load model parameters. Deterministic optimization methods heavily depend on a good initial estimate of the control variables, and poor estimates can result in the divergence of the optimization process. A component-based approach combined with knowledge of parameters of typical motors and system loads can help develop a baseline model that can be used as a starting point for the measurement-based approach. A recommended two-step process is as follows:

1. Use a component-based approach to get a baseline estimate of the percentages (*Fma, Fmb, Fmc, Fmd, Fel*) of the different components of the load model. An initial parameter set (physical parameters like r and x, time constants and typical protection settings) for the different load components can be derived by inspecting data sheets of commonly used motor types or by testing load components in a laboratory setting.
2. When an appropriate measurement for an event is made available, the developed baseline model in step 1 should be parameterized by using either manual tuning or an optimization technique.

Applying proper engineering judgement is crucial in the measurement-based approach. A prior working knowledge of linear systems, basic optimization, and sensitivity analysis is required as the composite load model has a complex mathematical structure. Due to the nature of the load it represents, the composite load model has multiple components (e.g motor A, B and C) with similar responses in certain operation ranges. As such, engineering judgement and knowledge of load responses is needed to assign appropriate bounds to the parameters that are being tuned. Without appropriate bounds on the parameters, the optimization method may either diverge or provide unrealistic values for certain parameters. This can often lead to a model being able to replicate one specific event but fail to replicate other events. There may also be issues with poor conditioning of the problem, leading to divergence of the optimization problem. The trick there is to optimize only a few parameters and fix the remaining based on engineering judgement and device knowledge. In addition to this, the protection parameters should not be tuned by any automatic optimization technique. Protection components like relays and contactors induce non-linear abrupt transitions in the load model. Optimization techniques that typically work on the principles of linear analysis are therefore not appropriate for tuning these parameters. These

parameters should be strictly tuned based on survey of common protection settings and experiences of load loss during measured grid events. A detailed treatment of these topics is beyond the scope of this document. The readers are encouraged to refer [3, 4, 14] for an in-depth discussion on these topics. Table 4-5 lists some of the recommendations for tuning the different parameters of the composite load model.

It is extremely important to note that all best efforts made to determine a reasonable composite load model parameterization (component + measurement based) in the end will still not be the definitive load model. This is because the load is constantly changing, and moreover, there will always be uncertainties in any and all methods. Therefore, some suitable sensitivity analysis is key in any planning study, and should be based on engineering judgment to identify the parameters to which the particular system and conditions being studied are sensitive too, and coming up with physically meaningful and reasonable range of sensitivities to study relative to those parameters. This will then help to gauge how uncertainties in the load model parameters may affect system performance.

Table 4-5
Recommendations for load model parameter derivation

Percentage composition	
Fma, Fmb, Fmc, Fmd, Fel, Z, I, P	The base values of these parameters should be generated using the **component-based approach** and these can be fine-tuned using the **measurement-based approach** using a least square error minimization or equivalent optimization method
Motor A, B, and C inductances, load characteristic and inertia	
LF, Ra, Ls, Lps, Lpps, Tpo, Tppo, H, Etrq,	Typical values for these parameters should be chosen based on NEMA type category, motor size and end load type. A limited tuning of these parameters can be done with the **measurement-based approach** using a least square error minimization or equivalent method, however, if such an exercise is done extreme care should be taken to ensure the derived tuning does not lead to physically meaningless motor characteristics. In general, it is not highly recommended to tune these electrical parameters of the motors. If tuning is attempted, it should only be done **after a reasonable percentage composition has been established.**
Vstall, Tstall, Frst, Vrst	The base values of these parameters are to be determined based on lab tests of actual HVAC systems. These threshold values can be fine-tuned further based on event data. **However, a manual tuning process coupled with knowledge of compressor motor stalling and restarting is strongly recommended rather than an optimization-based method since these are thresholds that trigger step changes in the model behavior**

Table 4 5 (continued)
Recommendations for load model parameter derivation

Motor D parameters	
Rstall, Xstall	The base values of these parameters are to be determined based on lab tests of actual HVAC systems. These can be tuned further using a **measurement-based approach**. **These parameters are only to be tuned once a reasonable estimate of Fmd is established.**
Kp1, Np1, Kq1, Nq1, Kp2, Np2, Kq2, Nq2, Vbrk, CmpKpf, CmpKqf	These parameters are best left as is and **should not be altered**. These are based on lab testing of HVACs
Protection parameters	
Vtr1, Ttr1, Ftr1, Vrc1, Trc1, Vtr2, Ttr2, Ftr2, Vrc2, Trc2, Fuvr, vtr1, ttr1, vtr2, ttr2, Vc1off, Vc2off, VC1on, VC2on, Tth, Th1t, Th2t, Tv, Vd1, Vd2, Frcel	The base values are based on surveys and inspection of actual motors and HVACs deployed in the system. These parameters should be fine-tuned further based on event data. **However, a manual tuning process coupled with engineering judgment is strongly recommended rather than an optimization-based method since protection parameters trigger step changes in the model behavior.**

References

[1] A. Gaikwad, P. Markham, P. Pourbeik, "Implementation of the WECC Composite Load Model for utilities using the component-based modeling approach," *Proc. of IEEE T&D Exposition*, May 2016, Dallas TX.

[2] A. Maitra, A. Gaikwad, P. Pourbeik, D. Brooks, "Load model parameter derivation using an automated algorithm and measured data," *Proc. of the IEEE PES General Meeting, Pittsburgh*, July 2008.

[3] S. Son, S.H. Lee, D. Choi, K. Song, J. Park, Y. Kwon, K. Hur, J. W. Park, "Improvement of Composite Load Modeling Based on Parameter Sensitivity and Dependency Analyses," *IEEE Trans. on Power Systems*, vol. 29, no. 1, pp. 242-250, 2014.

[4] P. Mitra, V. Vittal, "Role of Sensitivity Analysis in Load Model Parameter Estimation," *Proc. of IEEE PES General Meeting*, July 2017, Chicago, IL.

[5] LCET Version 3.1 available online: http://membercenter.epri.com/abstracts/Pages/ProductAbstract.aspx?ProductId=000000003002015441

[6] PNNL Load model data tool, available online: https://svn.pnl.gov/LoadTool

[7] Residential Energy Consumption Survey, available online: https://www.eia.gov/consumption/residential/

[8] Residential Building Stock Assessment, available online: http://ecotope.com/project/2011-residential-building-stock-assessment/

[9] Commercial building energy consumption survey, available online: https://www.eia.gov/consumption/commercial/

[10] California commercial end use survey, available online: https://www.energy.ca.gov/data-reports/surveys/california-commercial-end-use-survey

[11] Wilcox, S. and W. Marion. 2008. *User's Manual for TMY3 Data Sets*, NREL/TP-581-43156. April 2008. Golden, Colorado: National Renewable Energy Laboratory.

[12] National oceanic and atmospheric administration, NOAA.org.

[13] Load model data processing and parameter derivation tool version 6.0, available online: https://www.epri.com/research/products/000000003002014658

[14] P. Mitra, V. Vittal, P. Pourbeik, A. Gaikwad, "Load sensitivity studies in power systems with non-smooth load behavior," *IEEE Trans. on Power Systems*, vol. 32, no. 1, pp 704 – 715, 2017

5
RECENT DEVELOPMENTS IN LOAD MODELING

Load modeling is an ongoing research area and different aspects of the composite load model is being updated to make the model more closely mimic the physical behavior of loads and to be more numerically stable for large scale computation. This chapter documents some of the latest developments in the load modeling research area that is focused towards developing the composite load model.

The *Motorc* or *Motor1ph* Model

Since the motor D component is a performance-based model, this model lacks the ability to capture certain aspects of the dynamic response of a single-phase HVAC unit. Some of the concerns raised with the usage of the motor D model are as follows:

1. Due to the algebraic nature, the motor D model abruptly transitions from a running to a stall condition, and from a stall to a run condition (for appropriate parameters). The abrupt transition of the motor D model in simulation studies may cause numerical issues or result in overly pessimistic or optimistic (depending on *Vstall* and *Tstall*) results. In reality however, the transition from run to stall and vice versa, depends on the machine flux, inertia, and the compressor load.

2. The motor D model presently does not capture the effect of reacceleration of HVAC units. Again, this is because of the limitations of the algebraic representation used in this model. In certain voltage stressed portions of the system, the inrush current drawn during motor reacceleration after a fault can result in secondary voltage dip. This effect cannot be adequately captured by the motor D model.

To address these issues, a different approach to modeling single phase HVAC units has been explored. This approach is known as the phasor-based modeling of a single-phase induction motor [2]. In this approach a phasor-based model, that explicitly represents the flux dynamics, motor inertia, and the load torque is created. A beta version of the model, known as *motorc* is available in GE PSLF™. This model is expected to be named *motor1ph* in future versions to avoid any confusion with the motor C component of the composite load model.

The next few sections, provides a background of the phasor modeling approach, and highlights the differences and similarities between the phasor model (*motor1ph*) and the performance model (Motor D or *ld1pac*).

Phasor modeling of single-phase induction motor

A detailed description of the *motor1ph* (*or motorc*) model, and the validation of this model based on laboratory measurements can be found in [2], [3]. This section provides an overview of the concept of phasor modeling pertaining to modeling of single-phase induction motor for positive sequence load flow studies. The concepts of phasor modeling of single-phase induction motor have been treated qualitatively in this section. The readers are encouraged to refer to [4] for a comprehensive quantitative treatment of this topic.

A simple way to understand phasor modeling is by drawing parallels with positive sequence modeling for three phase loads. For 3-phase machine modeling, the components in the *abc* frame of reference are converted into the synchronously rotating frame of reference called the *dq* frame, using the Parks transformations [5]. When the *d*-axis and the *q*-axis are chosen appropriately, the *d* or the *q* component (depending on how the axes are choses) forms an envelope of three phase waveform and are the positive sequence components. This is shown in Figure 5-1.

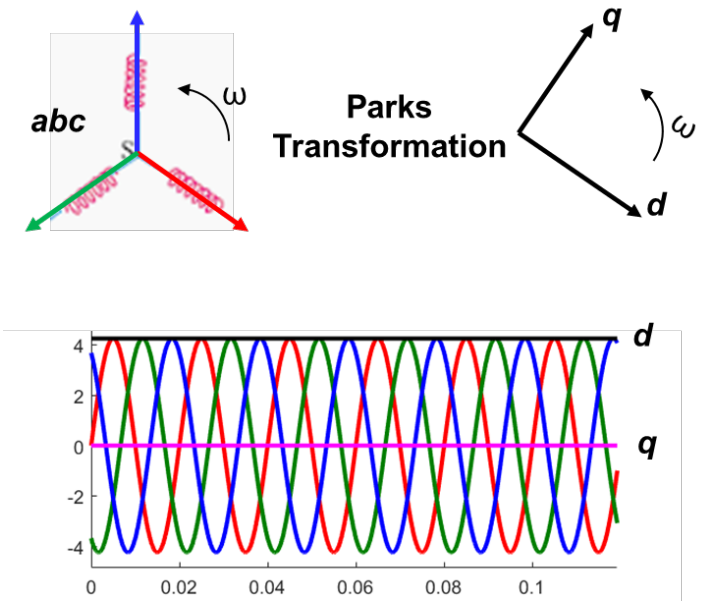

Figure 5-1
***abc-dq* transformation with d-axis and q-axis components on the abc waveform**

For single-phase systems, the Parks transformation is not applicable. Therefore, a phasor-based approach is chosen to capture the impact of single-phase machines in positive sequence studies. For a sinusoidal wave given by $Asin(\omega t+\phi)$, a phasor is defined as $A\angle\phi$ rotating at an angular speed of ω. This is shown in Figure 5-2. For any given waveform, the phasors at the component frequencies can be computed using the Fourier transform. For digital systems, this is achieved by using the discrete Fourier transformation. A more detailed analysis of phasors can be found in [2].

To create a phasor model of a single-phase induction motor, the rotor and stator quantities are converted from the rotor and stator frames, respectively to a single stationary frame. Since the new reference frame is stationary, the transformed quantities will still be stationary. This step is shown in Figure 5-3. After converting the rotor and stator quantities into the stationary rotating frame, the differential equations of flux and machine mechanics in the sinusoidal frame are converted into the phasor domain. The detailed equations of the single-phase induction motor, and the phasor domain equations can be found in [3]. The phasor domain quantities form the envelope of the sinusoidal waveform as shown in Figure 5-4. Finally, once the phasor model is created it is assumed that given *X* MW of single-phase induction motor on a load bus, the *X* MW is distributed evenly on the 3 phases (*X*/3 MW per phase). This final assumption makes sure that

the phasor quantities of the single-phase induction motor model are now equivalent to the positive sequence *dq* models of other 3-phase machines in the system.

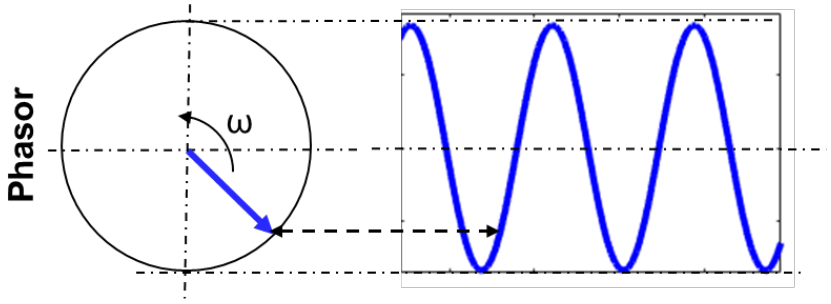

Figure 5-2
Phasor of a sinusoidal signal

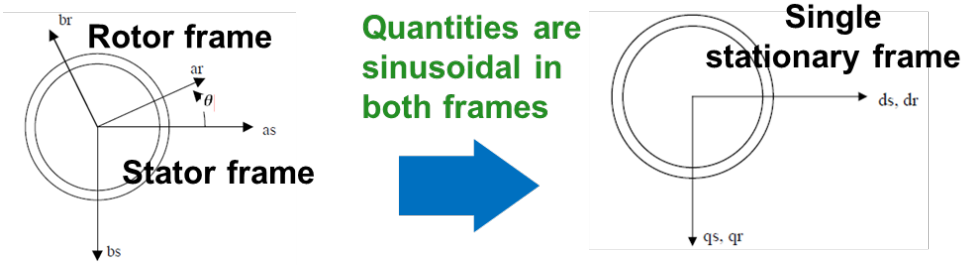

Figure 5-3
Conversion from rotor and stator frames to single stationary frame

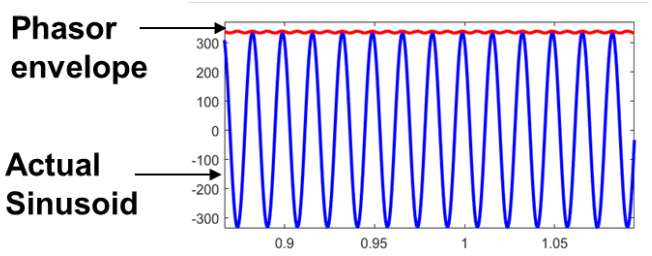

Figure 5-4
Actual sinusoid and phasor envelope

Comparison of the performance model with the flux-based phasor model of a single-phase induction motor

The motor D component of the composite load model is also available as a standalone model known as *ld1pac* in GE PSLF™. For the remainder of this discussion the performance model of the single-phase induction motor will be referred to as *ld1pac*. To compare the performance of the flux model *motor1ph* with the performance model *ld1pac* a test system as shown in Figure 5-5 is used. Different controlled waveforms were played in at the generator shown in Figure 5-5 and the differences and similarities in the transient behavior were noted.

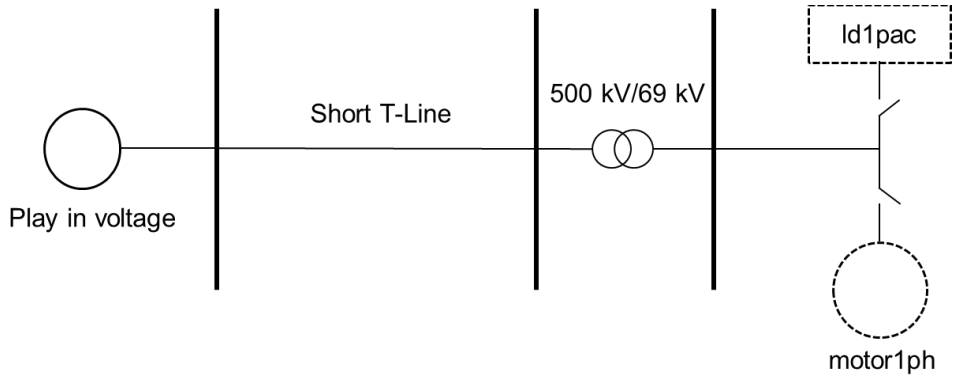

Figure 5-5
Test system for comparing the performance of *ld1pac* and *motor1ph*

Figure 5-6 shows the responses of the *ld1pac* and the *motor1ph* models for a 0.5 pu, 4 cycles sag the machine terminal. The *Vstall* and *Tstall* for *ld1pac* was set to 0.45 pu and 0.033s respectively. With these settings the *ld1pac* model is not expected to stall and should be in the running characteristics for the simulation. From Figure 5-6, it can be seen that the *motor1ph* model captures the impact of deceleration and acceleration on the active and reactive power consumption, while the *ld1pac* model does not capture this. The downward spikes in the blue curves for active and reactive power after the sag is impressed, accounts for the regenerative effect of the induction motor. The upward spikes in the blue curves for active and reactive power after the sag is removed, accounts for the reacceleration inrush of the induction machine. Although the transient responses of the two models differ, the steady state responses of both models were found to respond reasonably well.

Figure 5-7 shows the responses of the *ld1pac* and the *motor1ph* model for a 0.45 pu, 4 cycles sag at the terminals of the machine. As mentioned before the *Vstall* and *Tstall* for *ld1pac* was set to 0.45 pu and 0.033s, and the hence the *ld1pac* model goes into the stall state. For this simulation, frst was set to 1, such that all of the *ld1pac* restarts when the voltage recovers. A few interesting observations can be made from Figure 5-7. Some important observations are as follows:

1. The *motor1ph* model captures the regeneration transient at the inception of the sag, which the *ld1pac* does not capture. This again can be attributed to the modeling of the device flux inside the *motor1ph* model.

2. During the steady state running and the stalled condition, the *ld1pac* and the *motor1ph* models consume reasonably same amount of MW and Mvars. It should be noted that the models were approximately tuned to match each other in terms of steady state consumption. The *motor1ph* model can be tuned further to get a better match between the MW and Mvar consumption with *ld1pac* during running and stalled condition. Another important point to be noted here is that the inertia constant for the *motor1ph* model was set to 0.022. This value of inertia constant was chosen from [2]. The inertia constant of the *motor1ph* model has a strong influence on whether the model will go into a stall condition.

3. As the voltage recovers above the *Vrst* and *Trst* threshold, 100% of the *ld1pac* model goes back to the run state. However, the *motor1ph* model does not restart. After consultation with GE-PSLF™, it was understood that the *motor1ph* model is coded such that it does not restart

once the motor speed winds down to zero. The non-restarting behavior of this is not a physical limitation of the model, but an artifact of implementation in the software.

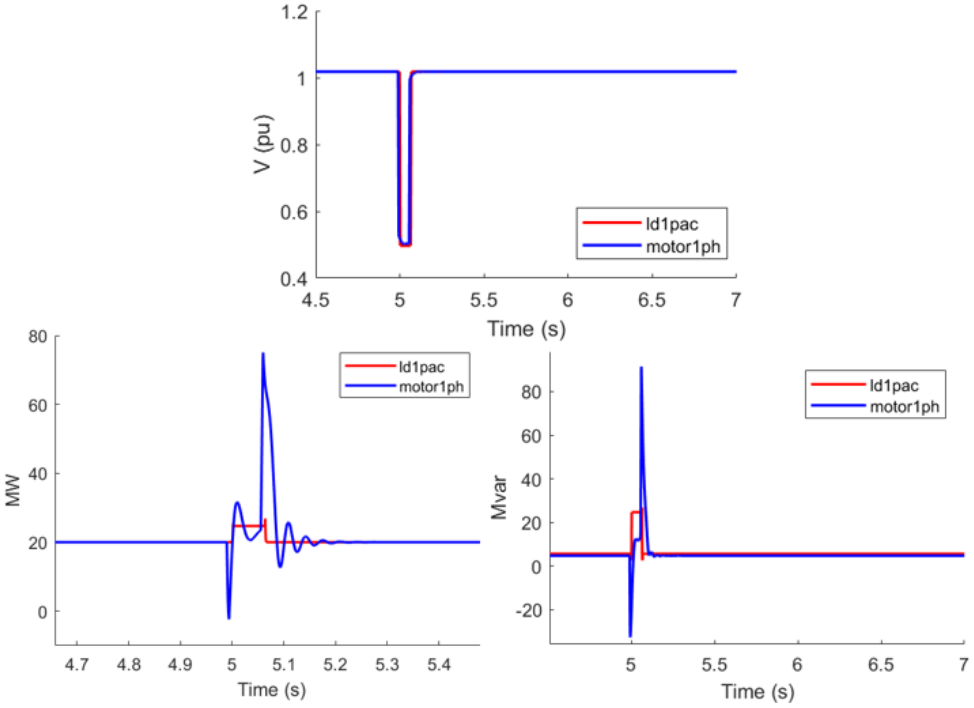

Figure 5-6
***ld1pac* and *motor1ph* response for a 0.5 pu 4 cyc sag**

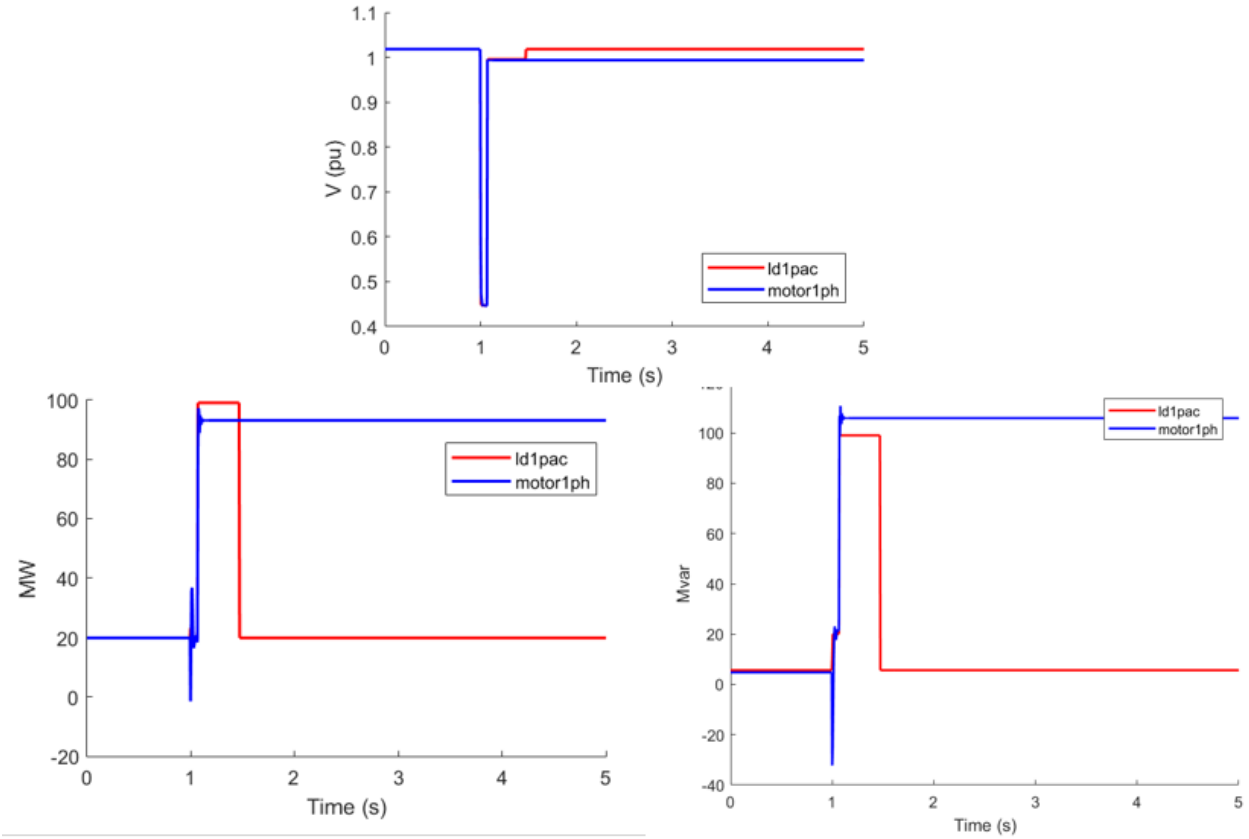

Figure 5-7
***ld1pac* and *motor1ph* response for a 0.45 pu 4 cyc sag with *frst* in *ld1pac* set to 1**

The responses of the *ld1pac* and the *motor1ph* model were also compared to the actual lab measurements of an HVAC unit with a 4 ton scroll compressor. To compare the responses, the test system shown in Figure 5-5 was modified slightly to match the lab setup. The modified one-line diagram is shown in Figure 5-8. With this set up, the *ld1pac* and the *motor1ph* models were setup and initialized such that the steady state power consumption matches approximately with the actual HVAC unit consumption. The same waveform that was used in the programmable power supply for the actual HVAC unit testing, was played in GE-PSLF™ using the waveform play-in model. The responses of the *ld1pac* and *motor1ph* models along with the actual test measurements were then plotted for comparison. It should be noted that for this comparison, the GE-PSLF™ models were not tuned to match the output obtained from the lab tests exactly. Rather, the goal of this exercise was to check whether the models could capture the different transients in an actual single-phase HVAC response.

Figure 5-9 shows the transient responses of the 4-ton HVAC unit, the *ld1pac* model, and the *motor1ph* model for a 0.5 pu, 4 cycles sag. The transient response region marked with red dotted ellipse has been elaborated in Figure 5-10 for a detailed discussion. In Figure 5-10, the regenerative effect, and the reacceleration inrush are marked with green and orange dotted boxes respectively. It can be seen that the *motor1ph* model (blue curve) captures the transient regeneration and reacceleration effects like the actual HVAC unit response. However, the *ld1pac* model (red curve) does not capture these transients in its response. Another important observation here is that the kvar response of the HVAC model does not match with the *motor1ph*

response during the reacceleration of the motor. This can be seen in the orange dotted box in the bottom plot of Figure 5-10. The *motor1ph* response indicates that the kvars drawn are inductive whereas the actual HVAC unit draws capacitive kvars. This is because the HVAC unit used for the lab testing had a separate starting capacitor that is connected using a speed voltage relay, and helps to produce a high locked rotor torque. The presence of the large starting capacitor results in the capacitive inrush current. The *motor1ph* model does not include a starting capacitor and hence the inrush current drawn is inductive.

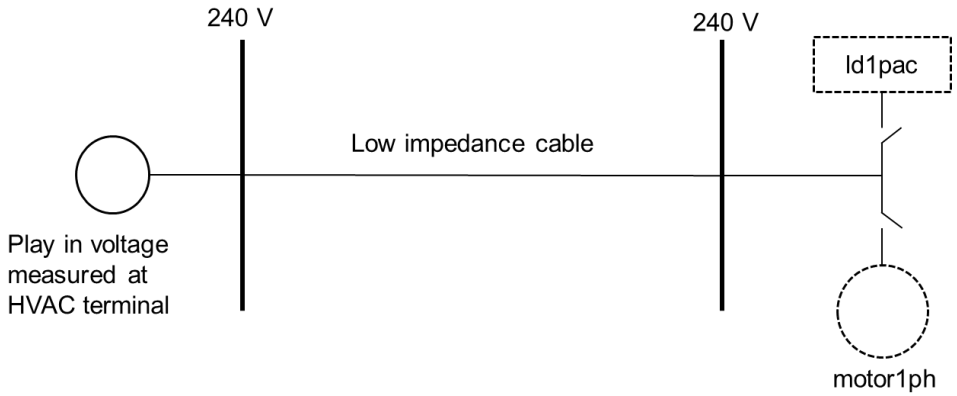

Figure 5-8
Modified one-line diagram replicating the test setup.

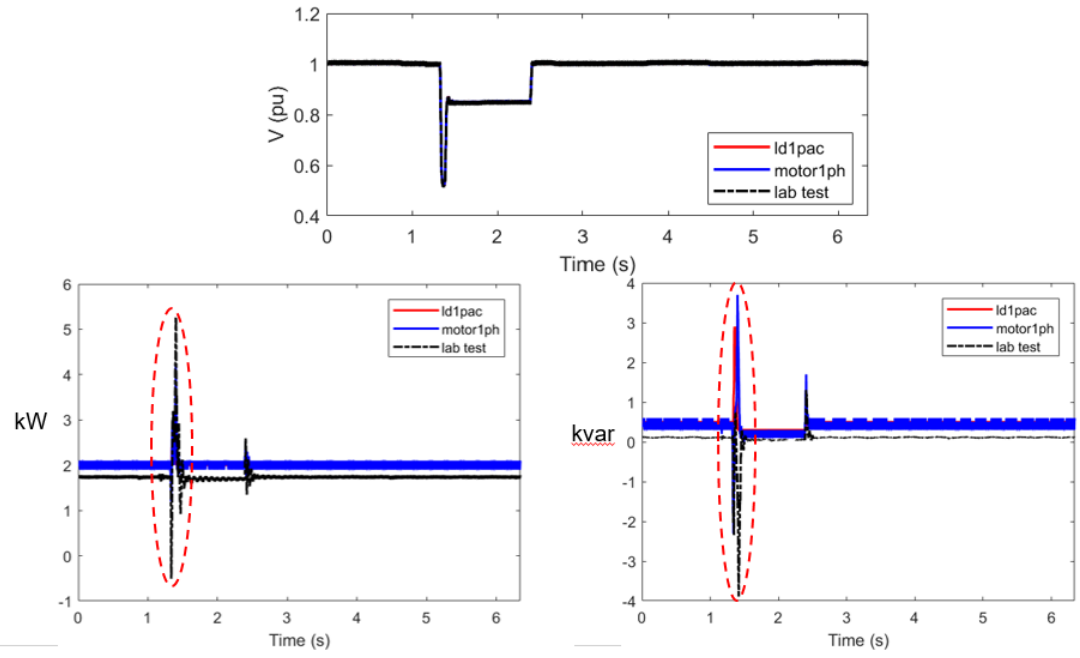

Figure 5-9
Comparison of the *ld1pac* and *motor1ph* model with lab test measurements of a 4 ton scroll compressor based HVAC unit, for a 0.5 pu, 4 cycles sag.

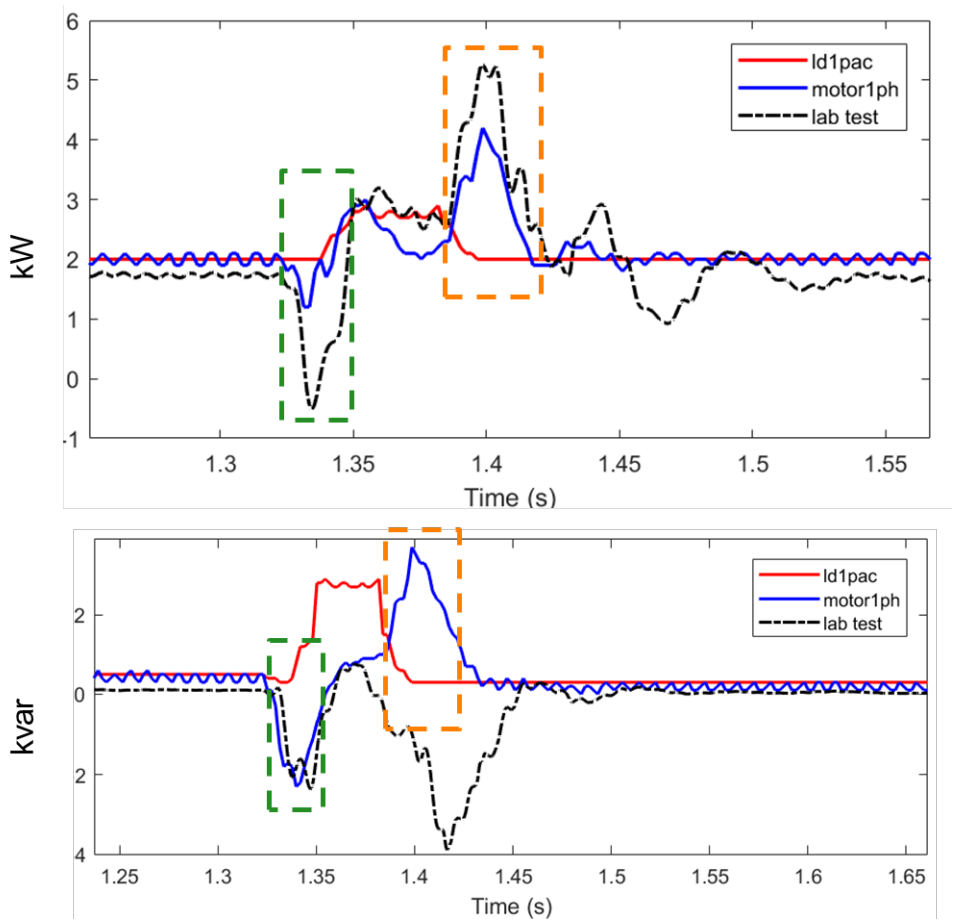

Figure 5-10
Detailed portion of the plot in Figure 5-9

Modeling improvements and future research

As shown here, the *motor1ph* model is a significant improvement in capturing some of the transient behaviors, that could not be captured by the *ld1pac* model. A comparison with an actual HVAC unit test also confirmed this. However, before drawing any sweeping conclusions about the effectiveness of the model, it should be recognized that for planning studies the goal is to develop a model that can capture the aggregated behavior of large number of loads. With this consideration the following concerns need to be addressed before the *motor1ph* model can be used for mainstream planning studies:

1. *Restarting capability*: Presently, the *motor1ph* model is implemented such that the model does not restart, once the speed of the motor is zero or close to zero. This implementation prevents the model from being used to represent HVAC units or a fraction of HVAC units that can restart. As shown in the previous chapter, most scroll compressors have the ability to restart from a locked rotor condition. Additionally, the *motor1ph* model does not have a representation of the starting capacitor. Without modeling a starting capacitor, the starting torque developed in the model may not be sufficient to overcome the load torque (if load torque is constant) preventing the motor from starting up. The restarting of the *motor1p* model may also be modeled by manipulating the load torque during start up conditions. These options will need to be evaluated such that it is possible to capture separate fractions of

motors having and lacking the ability to restart. Furthermore, these responses will need to be validated against the aggregated responses of a distributed group of HVAC units.

2. *Modeling inrush*: As shown in this chapter, the main advantage of the *motor1ph* model is its ability to model transient inrush behavior, and its transition between run and stall conditions based on the physics of the underlying motor. The ability to model inrush is important for capturing the transient voltage dips observed in voltage stressed portions of the system resulting from motor reacceleration. However, it should be recognized that the *motor1ph* model was developed based on lab measurements of a single HVAC unit. Therefore, modeling a large portion of the load at a bus using the *motor1ph* model may result in significantly higher than expected inrush current being drawn at those buses. This is because as the model represents synchronized reacceleration of all HVACs at a bus, which does not or rarely happen. Considering this, the issue of inrush modeling needs to be researched from the perspective of aggregated response of HVAC before using the *motor1ph* model for simulation studies.

Enhancement to the Stall Behavior of the Motor D Model

The composite load model (CMLD) uses a performance model for representing single phase induction motors driving reciprocating and scroll compressors in residential air-conditioning and refrigeration systems. These motors are prone to stall and have shown to have significant impact on voltage recovery following transmission faults. The performance model makes a switch from motor "run" to "stall" state based on a single definite-time threshold represented with "Vstall" and "Tstall" parameters in the model. This representation may be adequate for estimating motor stalling during a transmission fault. However,

a. Testing performed by EPRI and BPA as well as recent analytical work found that motor stalling follows an inverse-time characteristic, and

b. Studies performed by EPRI and NERC found that modeling the time-dependence of stalling is important for capturing motor stalling in weak transmission systems.

To address these issues and inverse-time "Vstall-Tstall" curve for use in simulation studies to gain a better representation of HVAC stalling during voltage sags was proposed in 2019.

Proposal

Based on the air-conditioner testing data from EPRI and BPA, in 2019, the NERC LMTF recommended the inclusion of a "Vstall-Tstall" characteristic for stall transition in the motor D model *in addition to* the existing logic. The characteristic is listed in Table 5-1 and shown in Figure 5-11. This implementation at present will be hard coded within the composite load model and will be activated when the user supplies a negative value for tstall in the dynamic data file.

Table 5-1
Proposed values of Vstall and Tstall for inverse time stall characteristic representation

Tstall (cycles)	Vstall (pu voltage)
2	0.45
3	0.49
6	0.51
9	0.53
12	0.55
15	0.565
No stall (9999)	V>0.565

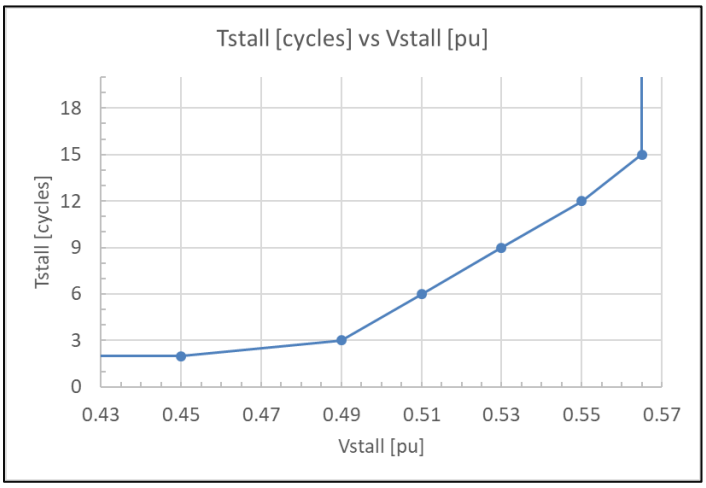

Figure 5-11
Inverse time Vstall-Tstall characteristic

Background for this enhancement

Over the past few years, BPA and EPRI have conducted a series of tests on single-phase residential HVAC systems driven by scroll or reciprocating compressors in the past few years. The goal of these tests was primarily to determine the relationship between the level and duration of a voltage sag (Vstall and Tstall) that would cause a residential HVAC compressor motor to stall. To perform these tests, a set of programmed voltage sags were applied for fixed durations at the terminals of the HVAC units to determine the type of sag that would result in the stalling of the HVAC unit. Figure 5-12 shows a sample voltage sag that was used for these tests. Note that the waveform is shown in Figure 5-12 is an example and the voltage sag level and duration were varied during the tests. Figure 5-13 shows the Vstall and Tstall characteristics recorded by BPA during the tests conducted in the BPA testing facilities [6].

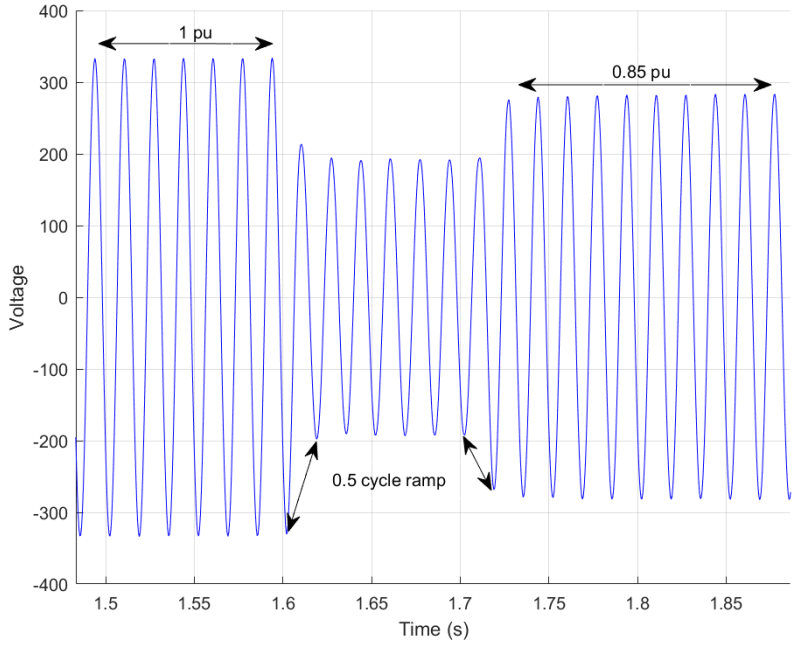

Figure 5-12
Sample voltage dip impressed at the terminal of the machine

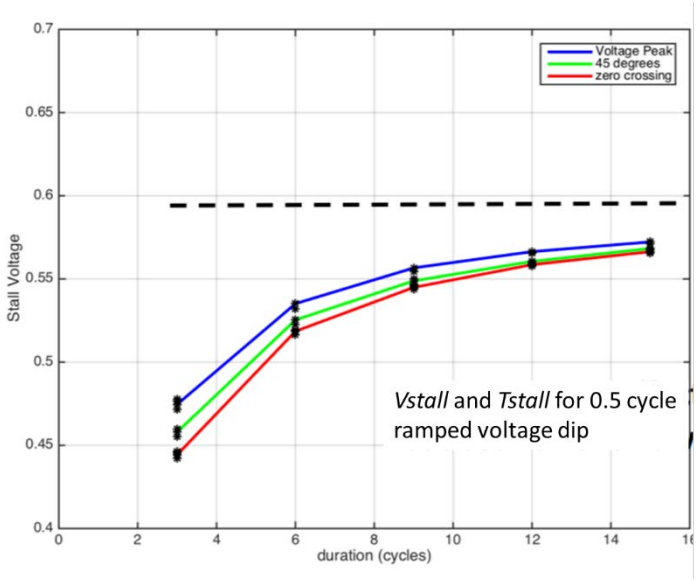

Figure 5-13
Vstall vs. Tstall characteristics for single phase residential scroll/reciprocating compressor equipped HVAC system tested by the BPA [1]

Based on results shown in Figure 5-13, GE PSLF ™ has a time dependent stall characteristic implemented in the single-phase HVAC model *ld1pac* [7]. The Vstall vs. Tstall characteristic hard coded in PSLF is as shown in Figure 5-14.

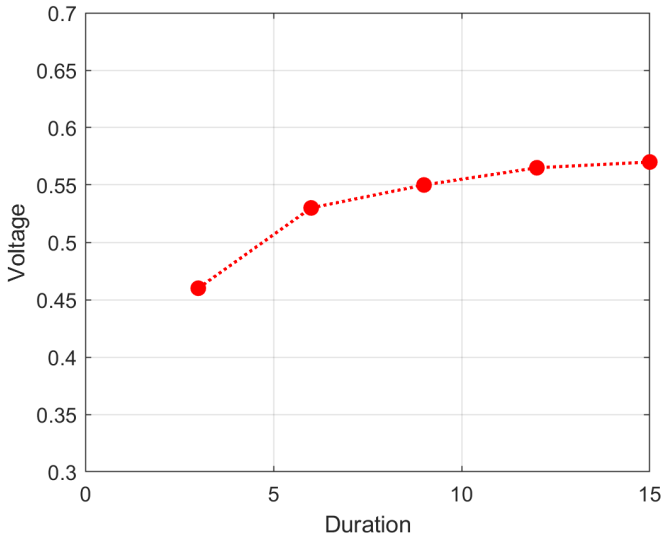

Figure 5-14
Vstall vs. Tstall characteristics hard-coded in the GE PSLF™ *ld1pac* model [2]

EPRI conducted a series of HVAC tests in 2010 for the Arizona Public Service and SRP, and some more tests between 2016-2018 [8], [9]. These tests were repeated at different ambient temperatures to identify the impact of the ambient temperature variation on the stalling of HVAC compressors. Figure 5-15 – Figure 5-17 shows the Vstall vs. Tstall characteristics recorded during these. The bold black lines in these plots show the average Vstall vs. Tstall characteristic of all the tested HVAC units at the respective ambient temperatures. Note that, the legend notation "Armstrong4TR22R" indicates that the tested unit is a 4-ton Armstrong unit with R22 refrigerant and a reciprocating compressor.

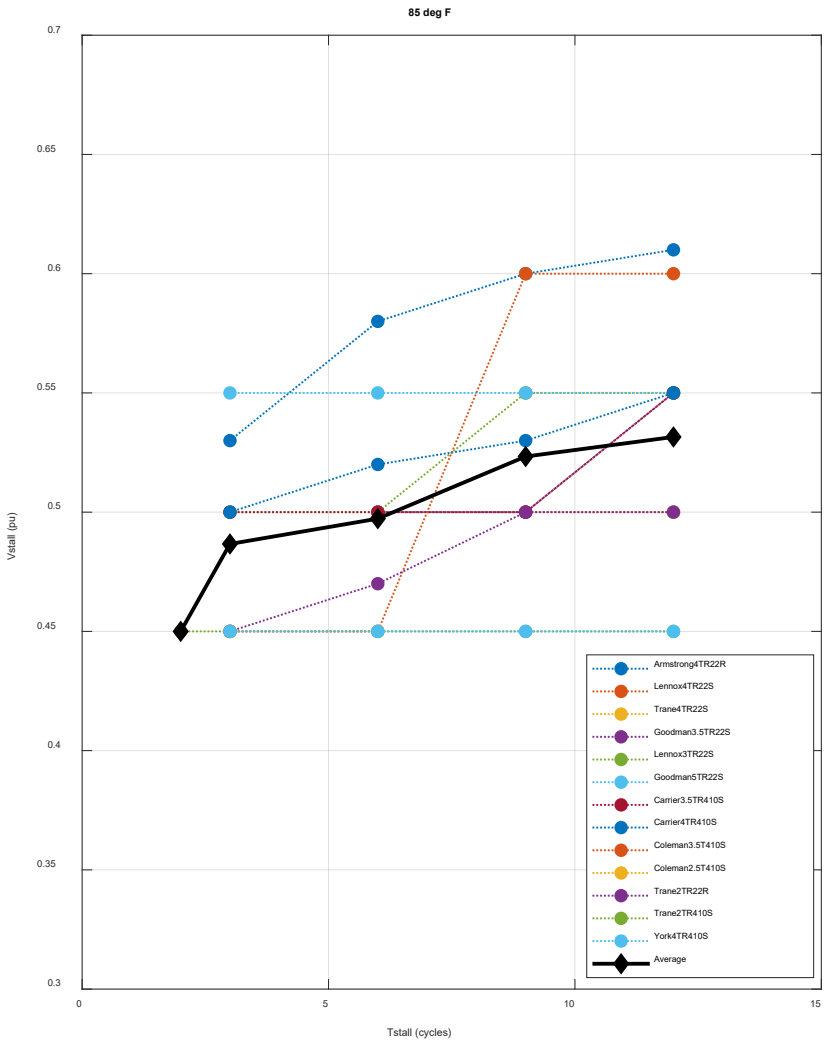

Figure 5-15
Vstall vs. Tstall characteristics of different HVAC units tested by EPRI at 85 deg F

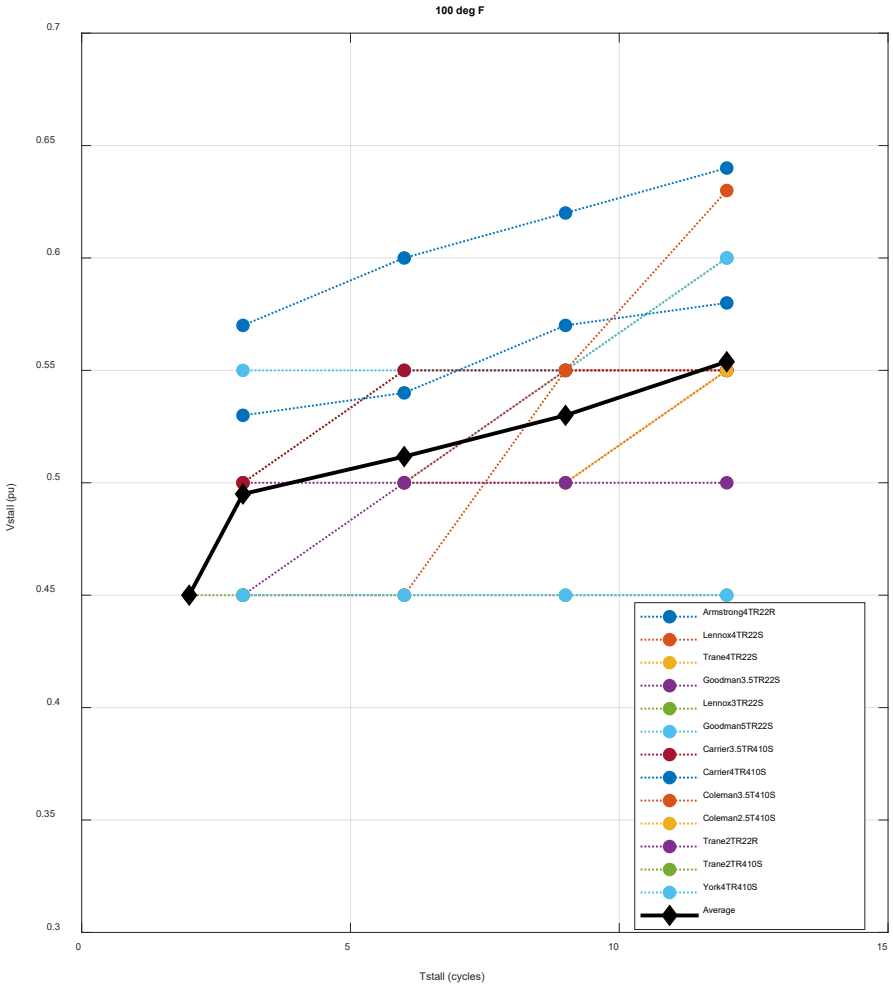

Figure 5-16
Vstall vs. Tstall characteristics of different HVAC units tested by EPRI at 100 deg F

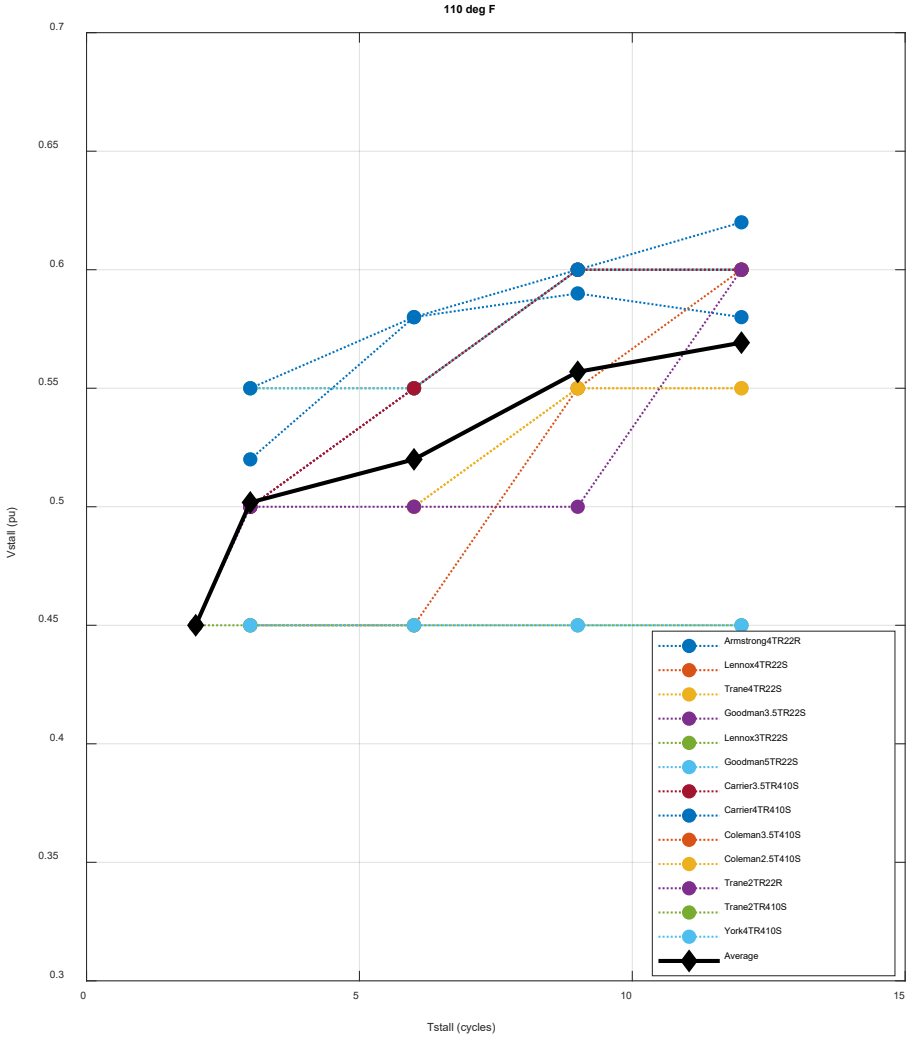

Figure 5-17
Vstall vs. Tstall characteristics of different HVAC units tested by EPRI at 110 deg F

To better visualize the different recorded Vstall vs. Tstall characteristics, the average characteristics (bold black curve) in Figure 5-15 - Figure 5-17 and the characteristics in Figure 5-14 are plotted together in Figure 5-18. The data points corresponding to Figure 5-18 are summarized in Table 5-2. The numerical values provided in Table 5-2 can be used as a guide for finalizing the time dependent stall behavior, which shall complement the existing logic for stall implementation in the motor D model.

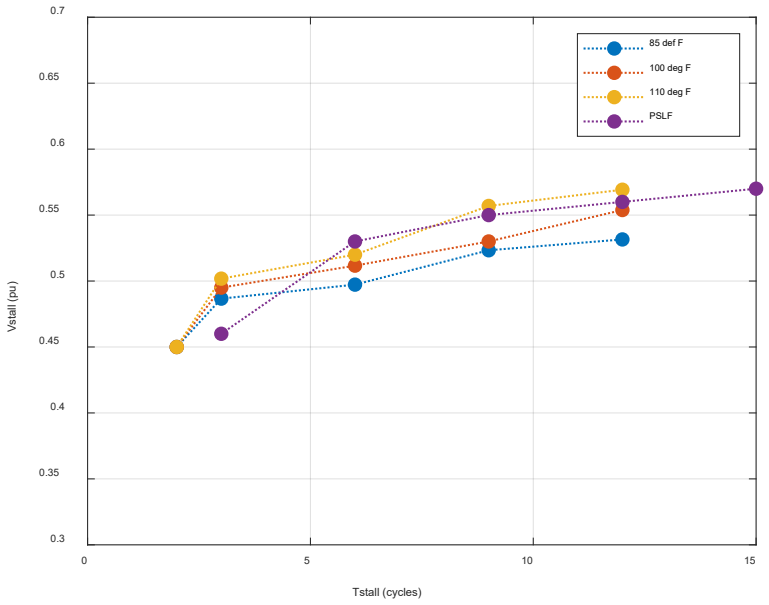

Figure 5-18
Combined plot for Vstall vs. Tstall characteristics

Table 5-2
Vstall vs. Tstall (average characteristics)

Tstall (cyc)	EPRI (85 deg F)	EPRI (100 deg F)	EPRI (115 deg F)	PSLF
	Vstall			
2	0.45	0.45	0.45	NA
3	0.48	0.49	0.50	0.46
6	0.49	0.51	0.52	0.53
9	0.52	0.53	0.56	0.55
12	0.53	0.55	0.57	0.565
15	NA	NA	NA	0.57

New Variable Speed Drive Model

In 2017, six variable frequency drives of different ratings across two manufacturers were tested in the lab at EPRI [10]. The aim of the tests was to characterize and observe behavioral trends of the drives, with default out of the box settings, to voltage sags of varying depth and duration. The assumption was that the use of these default out of the box settings would be the norm for a majority of drive interfaced loads connected on the power system.

An inspection of the measurement data revealed that the power electronic component shown in Figure 3-11 may not be able to adequately capture the response of variable speed drives, which have a significant difference in dynamic response as compared to common household electronic loads. To address this, the measurement data from the lab tests were used to develop a new

positive sequence model meant to represent the aggregated response of variable speed drives connected downstream of a distribution substation. In 2018, based upon discussions at the WECC model validation working group (MVWG) a model structure was finalized.

Modeling approach

The block diagram for the proposed model is shown in Figure 5-19. The model utilizes 2 states associated with 2 washout blocks to capture the response of VFDs as observed from the laboratory test measurements. The washout blocks, with the limiters, are used to accurately capture the effect of:

1. reverse biasing of drive diodes during a terminal voltage sag, and
2. the inrush drawn by the VFD during the terminal voltage recovery/increase.

During a voltage sag, the diodes at the front end of the drive get reverse biased causing the current drawn by the drive to drop until the internal capacitor discharges into the end load and the diode becomes forward biased again (if it does). This results in the active and reactive power to drop first and then slowly rise back (like a washout action). When the voltage recovers after the sag the partially discharged capacitor now draws an inrush causing the active and reactive power to rise first and then slowly go down to the steady state value (again like a washout action). Upon voltage recovery, the magnitude of inrush current drawn by the model is limited by the limiters.

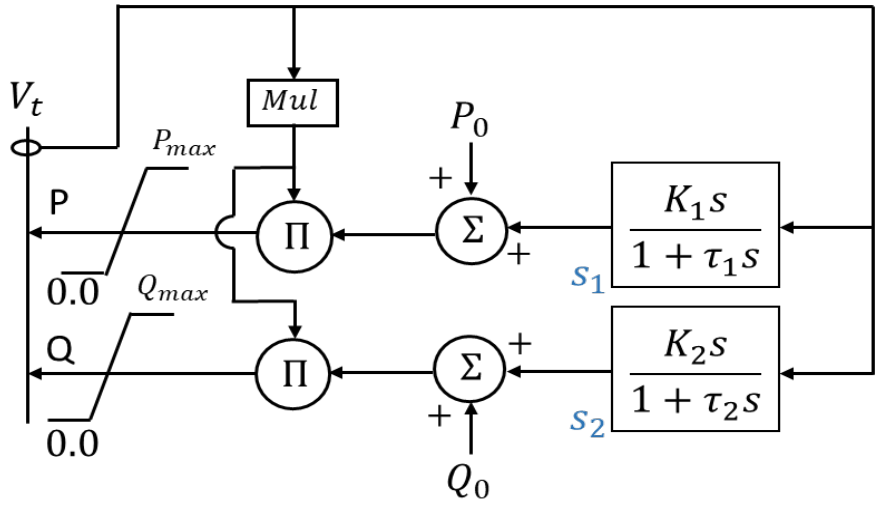

Figure 5-19
Block diagram of modeling approach

The parameter and variable list for this modeling approach is tabulated in Table 5-3. Internal to the model, the actual values of active and reactive power limits are calculated as

$$P_{\max\_internal} = P_{max} * P_0 * Mul$$
$$Q_{\max\_internal} = Q_{max} * Q_0 * Mul \quad \text{(Eq. 5)}$$

It is important to mention that as of preparation of this document, this model is yet to be included in any commercial power system simulator. Certain aspects of the model are expected to change during the course of implementation and benchmarking of the model.

Table 5-3
Parameter and variable list

Name	Description	Sample Value
V_t	Terminal voltage (pu)	Input
K_1	Washout gains for active power	0.8
τ_1	Time constants for active power (s)	0.2
K_2	Washout gains for reactive power	0.03
τ_2	Time constant for reactive power (s)	0.05
Mul	Multiplier value from partial trip characteristic	Obtained from partial trip block (see Figure 5-22)
P_{max}	Maximum value of active power (pu)	1.1
Q_{max}	Maximum value of reactive power (pu)	1.1
P_0	Steady state load active power (pu)	Evaluated during initialization
Q_0	Steady state load reactive power (pu)	Evaluated during initialization

Representative results

Lab tests were performed on drives from two manufacturers with the ratings of:

1. Manufacturer 1: 30 HP – 480V line – line.
2. Manufacturer 2: 30 HP – 480V line – line.
3. Manufacturer 2: 30 HP – 240V line – line.
4. Manufacturer 2: 60 HP – 480V line – line.
5. Manufacturer 2: 125 HP – 480V line – line.
6. Manufacturer 2: 100 HP – 480V line – line.

The different voltage sags that were used to test the drives are defined in Table 5-4.

Table 5-4
Lab tests run on the drives

Depth	Duration
0.95pu	120 cycles
0.9pu	120 cycles
0.85pu	120 cycles
0.8pu	120 cycles
0.75pu	120 cycles
0.7pu	8 cycles
⋮	⋮
0.5pu	8 cycles
0.5pu	120 cycles or until trip
⋮	⋮
0.2pu	8 cycles
0.2pu	120 cycles or until trip

From the tests conducted, a profile of the trip characteristic was constructed as shown in Figure 5-20.

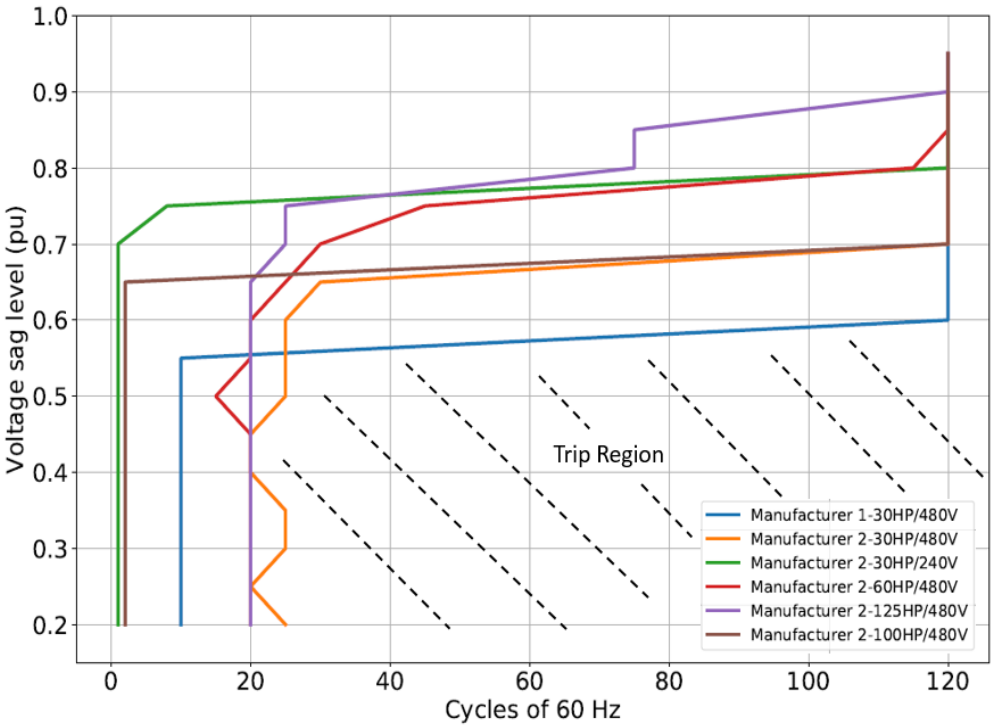

Figure 5-20
Profile of trip characteristic

The characteristics can also be constructed as shown in Figure 5-21 for specific sag durations. The values on y axis of this figure are calculated as the ratio of sum of the ratings of the drives that were able to ride through the sag to the sum of ratings of all drives used in the tests.

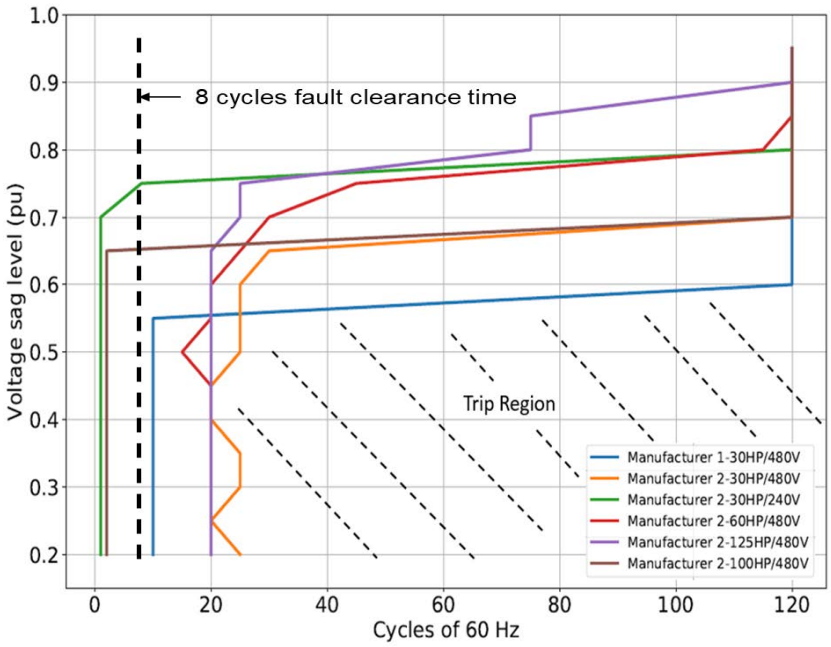

Figure 5-21
Trip characteristics for specific sag durations

The total horsepower rating of all drives tested is 375 HP ((30*3) + 60 + 125 + 100). Assuming a generic 8 cycle fault clearing time, Table 5-5 can be constructed.

Table 5-5
Derivation of per unit ride through parameter values

Sag level (pu)	Drive tripped (HP)	Per unit of ride through
V_{sag} > 0.75pu	0	375/375 = 1.00pu
0.65 < V_{sag} < 0.75	30	340/375 = 0.91pu
V_{sag} < 0.65	30 + 100 = 130	245/375 = 0.65pu

Based on these observed trip characteristics, the partial trip characteristic was setup as shown in Figure 5-22 with parameter values as tabulated in Table 5-6. The structure of this partial trip characteristic is the same as the one included in the recently approved aggregated distributed energy resource *der_a* model [11]. A detailed version of the aggregated VFD model can be found in [12].

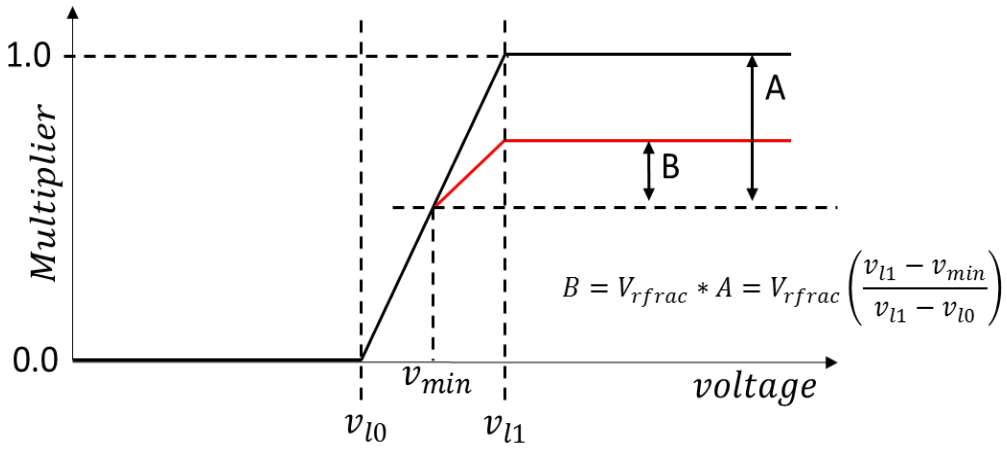

Figure 5-22
Partial trip characteristic

Table 5-6
Parameter description for partial trip characteristic

Name	Description	Sample Value
v_{l0}	Low voltage threshold 0 (pu)	0.55
tv_{l0}	Timer associated with v_{l0} (s)	1.05
v_{l1}	Low voltage threshold 1 (pu)	0.75
tv_{l1}	Timer associated with v_{l1} (s)	0.13
V_{rfrac}	Fraction of drives remaining online	0.65

To compare the performance of the model with the test results, the model was constructed as standalone equations in Python. Some of the comparative results of the models and the test data are shown in Figure 5-23 – Figure 5-26. The legend entry PSLF refers to the response of the power electronic component in the composite load model.

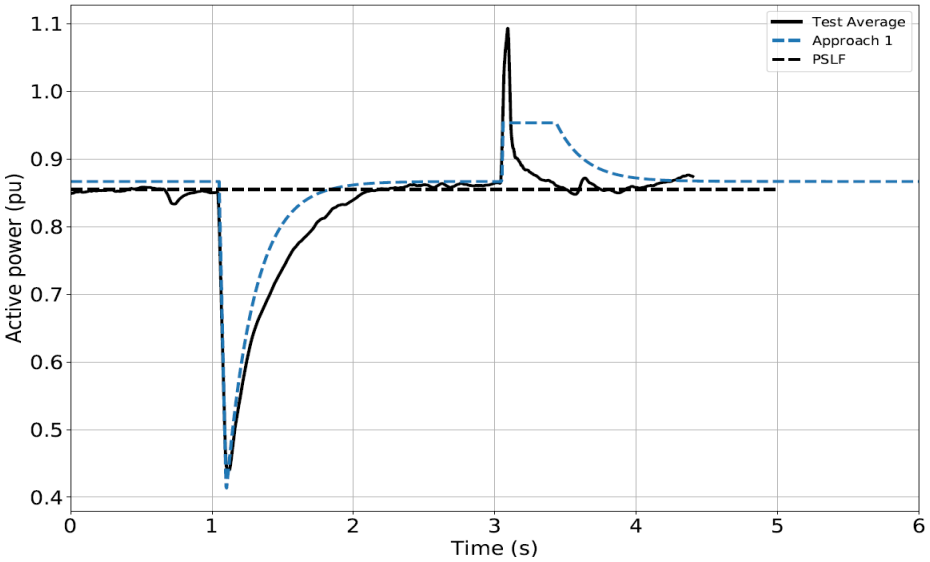

Figure 5-23
Comparison of active power for a 120 cycle 0.9pu voltage sag

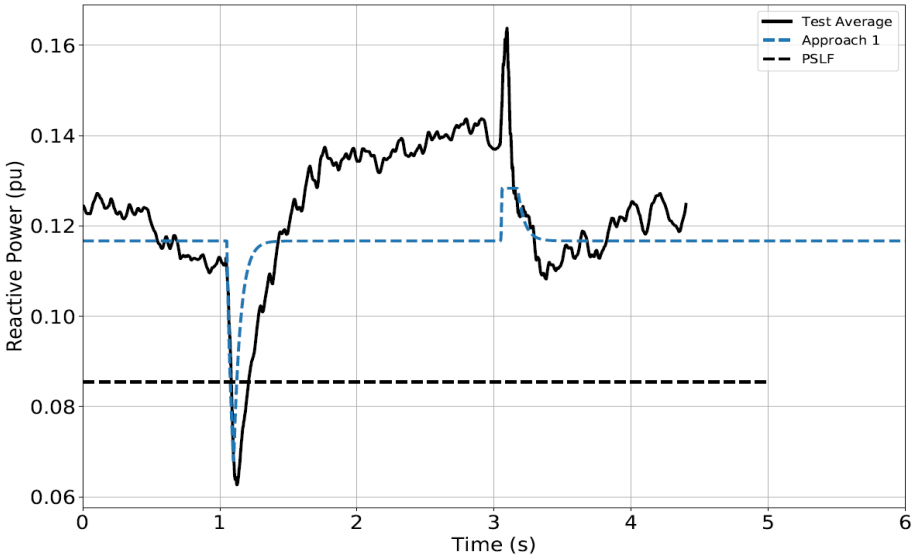

Figure 5-24
Comparison of reactive power for a 120 cycle 0.9pu voltage sag

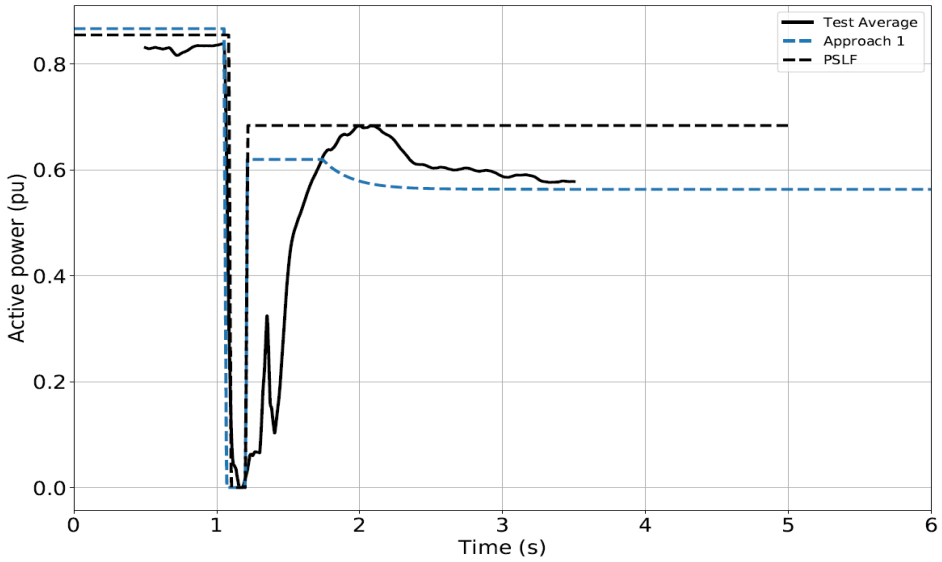

Figure 5-25
Comparison of active power for an 8 cycle 0.4pu voltage sag

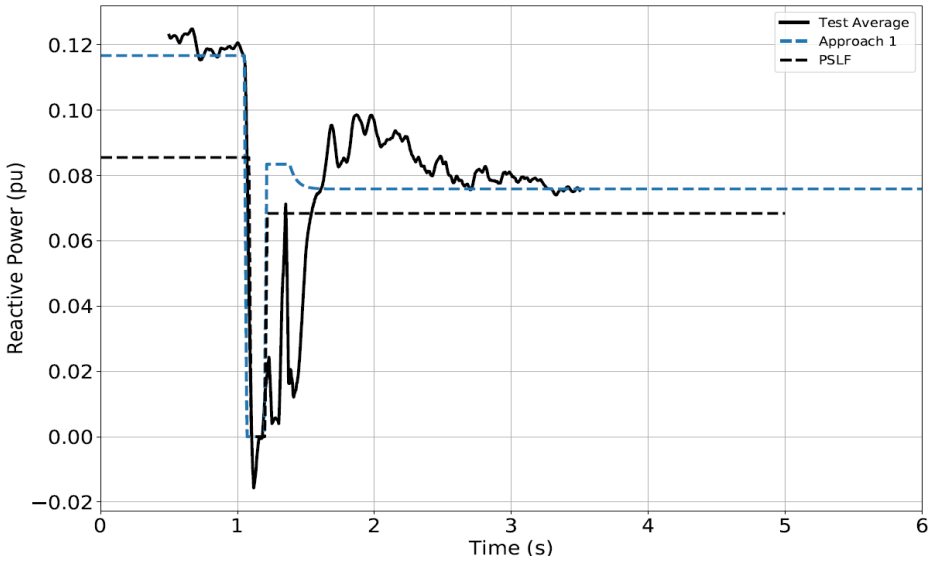

Figure 5-26
Comparison of reactive power for an 8 cycle 0.4pu voltage sag

References

[1] *Load characteristics LD1PAC,* Powerworld documentation, available online: https://www.powerworld.com/WebHelp/Content/TransientModels_PDF/Load/Load_Characteristic/Load%20Characteristic%20LD1PAC.pdf

[2] B. Lesieutre, D. Kosterev, J. Undrill, "Phasor modeling approach for single phase A/C motors," *Proc. of 2008 IEEE PES General Meeting*, 20-24 July 2008.

[3] *Load modeling transmission research*, prepared for CIEE by LBNL, available online: https://web.eecs.umich.edu/~hiskens/publications/LM_Final_Report.pdf

[4] A. M. Stankovich, B. Lesieutre, T. Aydin, "Modeling and analysis of single-phase induction machines with dynamic phasors," *IEEE Transactions on Power System*, vol. 14, no. 1, pp. 9-14, 1999.

[5] P. Kundur, *Power system stability and control,* McGraw Hill publications.

[6] End Use Testing at BPA, NERC-DOE FIDVR Workshop, available online: http://eta-publications.lbl.gov/sites/default/files/4d-kosterev-end-use-testing-at-bpa.pdf

[7] GE PSLF ™ User manual

[8] *Technical Update on Load Modeling*: EPRI, Palo Alto, CA: 2017. 3002010754.

[9] *Technical Update on Load Modeling*: EPRI, Palo Alto, CA: 2018. 3002013562.

[10] *Technical Update on Load Modeling*: EPRI, Palo Alto, CA: 2017. 3002010754.

[11] *The New Aggregated Distributed Energy Resources (der_a) Model for Transmission Planning Studies*: EPRI, Palo Alto, CA: 2018, 3002013498.

[12] P. Mitra, D. Ramasubramanian, A. Gaikwad, J. Johns, "Modeling the aggregated response of variable frequency drives (VFDs) for power system dynamic studies," *IEEE Trans. On Power System,* vol. 35, no. 4, pp 2631 – 2641, July 2020.

A
COMPOSITE LOD MODEL COMPONENTS

Dynamic model of 3 phase induction motors (Motor A, Motor B and Motor C)

The block diagram of the 3-phase induction motor modeled in PSLF™ is shown in Figure A-1. The block diagram of the 3-phase induction motor modeled in PSS®E is shown in Figure A-2. The models in PSLF™ and PSS®E are slightly different, in that, PSS®E uses a leakage impedance, whereas the PSLF™ models makes an approximation and does not require this quantity. Presently, PSS®E does not require the leakage reactance Xl as an input from the user and assumes Xl as 0.8 Lp. Powerworld has the option of handling both these models in its Powerworld Simulator.

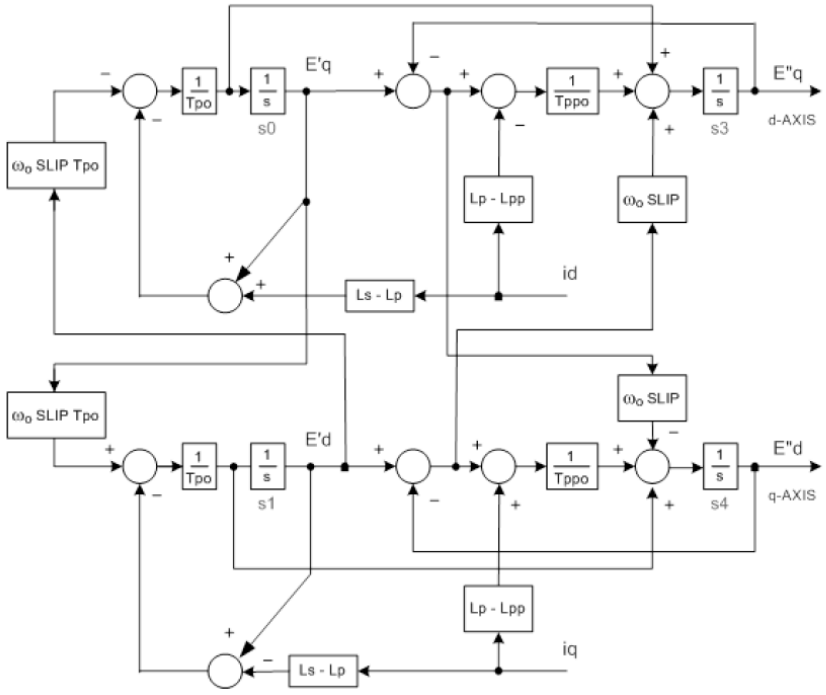

Figure A-1
Block diagram of PSLF motorw model used to model motor A, B and C in the composite load model (Source: GE PSLF™ User Manual)

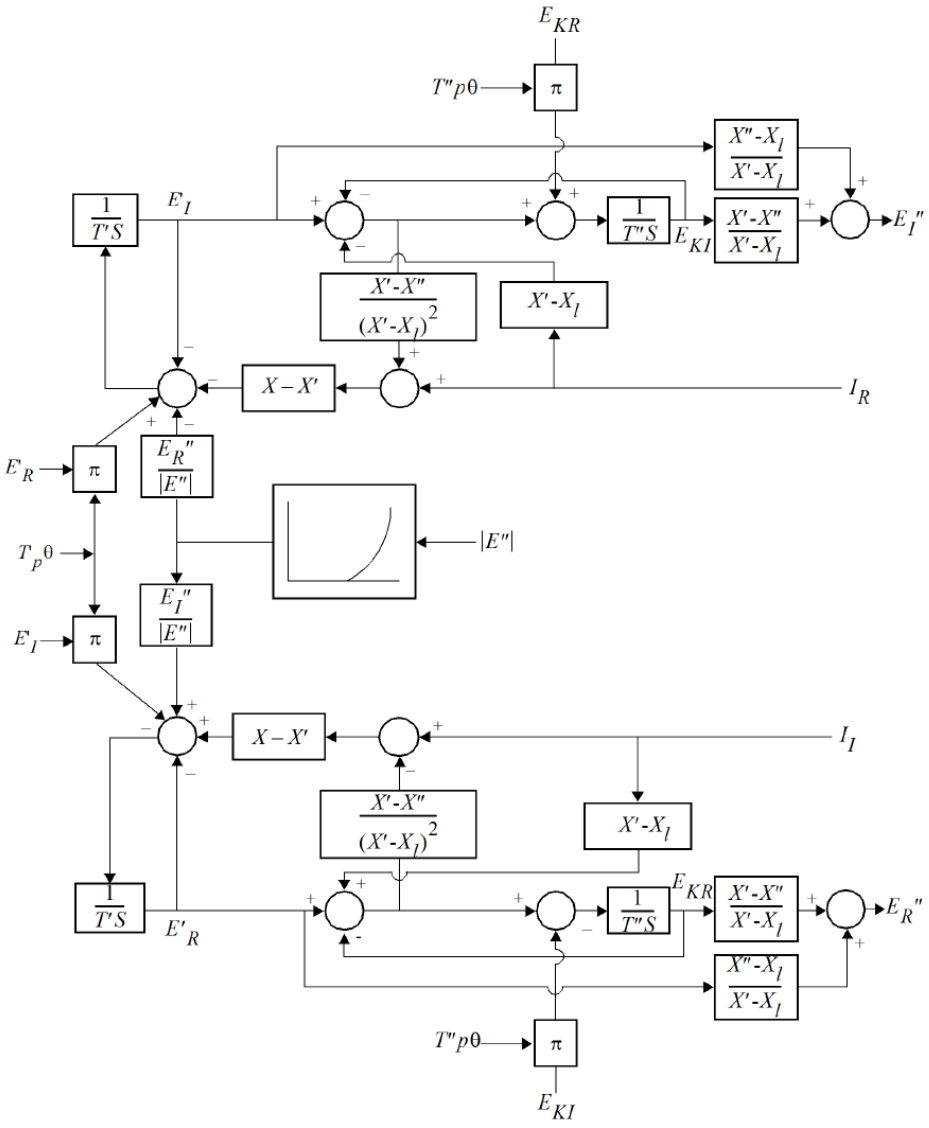

Figure A-2
Block diagram of PSS®E induction motor model used to model motor A, B and C in the composite load model (Source: Siemens PTI PSS®E Program Application Guide Volume II)

The equations for the 5th order model based on Figure A-1 is as follows:

$$\frac{dEq'}{dt} = -\frac{1}{Tp0}[Eq' + (Ls - Lp)id] - \omega 0 \cdot s \cdot Ed' \quad \text{(Eq. A-1)}$$

$$\frac{dEd'}{dt} = -\frac{1}{Tp0}[Ed' - (Ls - Lp)iq] + \omega 0 \cdot s \cdot Eq' \quad \text{(Eq. A-2)}$$

$$\frac{dEq''}{dt} = \left(\frac{1}{Tpp0} - \frac{1}{Tp0}\right)Eq' - \left(\frac{Ls-Lp}{Tp0} - \frac{Lp-Lpp}{Tpp0}\right)id + \omega 0 \cdot (1 - Tp0) \cdot Ed' - \frac{1}{Tpp0}Eq'' - \omega 0 \cdot s \cdot Ed'' \quad \text{(Eq. A-3)}$$

$$\frac{dEd''}{dt} = \left(\frac{1}{Tpp0} - \frac{1}{Tp0}\right) Ed' + \left(\frac{Ls - Lp}{Tp0} - \frac{Lp - Lpp}{Tpp0}\right) iq + \omega 0 \cdot (1 - Tp0) \cdot Eq' - \frac{1}{Tpp0} Ed'' + \omega 0 \cdot s \cdot Ed" \quad \text{(Eq. A-4)}$$

$$\frac{ds}{dt} = -\frac{Ed''id + Eq''iq - Tm0\omega 0^{Etrq}}{2H} \quad \text{(Eq. A-5)}$$

$$id = \frac{Rs(Vd - Ed'') + Lpp(Vq - Eq'')}{Rs^2 + Lpp^2} \quad \text{(Eq. A-6)}$$

$$iq = \frac{Rs(Vq - Eq'') - Lpp(Vd - Ed'')}{Rs^2 + Lpp^2} \quad \text{(Eq. A-7)}$$

$$p3\emptyset = \frac{Rs(Vd^2 + Vq^2 - VdEd'' - VqEq'') - Lpp(VdEq'' - VqEd'')]}{Rs^2 + Lpp^2} \quad \text{(Eq. A-8)}$$

$$q3\emptyset = \frac{Lpp(Vd^2 + Vq^2 - VdEd'' - VqEq'') - Rs(VdEq'' - VqEd''))]}{Rs^2 + Lpp^2} \quad \text{(Eq. A-9)}$$

Dynamic model for Motor D

The performance-based HVAC model motor D has three distinct running states.

i. Region 1**:** Terminal voltage (V_t)> Compressor break down voltage (V_{brk}).

ii. Region 2**:** Stall Voltage (V_{stall}) <Terminal voltage (V_t) ≤Compressor break down voltage (V_{brk}).

iii. Region 3: Terminal voltage (V_t) ≤ Stall Voltage (V_{stall})

Region 1 and region 2 are running states, while region 3 represents the stalled condition of the AC model. The active and the reactive power consumed by the single-phase AC during the different running states are as follows:

i. Region 1

$$P_{run} = Kp1(V_t - V_{brk})^{Np1} + P_0 \quad \text{(Eq. A-10)}$$

$$Q_{run} = Kq1(V_t - V_{brk})^{Nq1} + Q_0 \quad \text{(Eq. A-11)}$$

ii. Region 2

$$P_{run} = Kp2(V_{brk} - V_t)^{Np2} + P_0 \quad \text{(Eq. A-12)}$$

$$Q_{run} = Kq2(V_{brk} - V_t)^{Nq2} + Q_0 \quad \text{(Eq. A-13)}$$

iii. Region 3

$$P_{stall} = V_t^2 G_{stall} \quad \text{(Eq. A-14)}$$

$$Q_{stall} = V_t^2 B_{stall} \quad \text{(Eq. A-15)}$$

Static Load Model

$$P = P_o\left(P1c\left(\frac{V}{Vnom}\right)^{P1e} + P2c\left(\frac{V}{Vnom}\right)^{P2e} + P3\right)(1 + Pf * Df)$$

$$Q = Q_o\left(Q1c\left(\frac{V}{Vnom}\right)^{Q1e} + Q2c\left(\frac{V}{Vnom}\right)^{Q2e} + Q3\right)(1 + Qf * Df)$$

$$P_o = Pload(1 - Fma - Fmb - Fmc - Fmd - Fel) \quad \text{(Eq. A-16)}$$

$$Q_o = P_o * acos(power\ factor)$$

$$P3 = 1 - P1c - P2c$$

$$Q3 = 1 - Q1c - Q2c$$

where,

P1c, Q1c	Fraction of constant current load with $P1e = 1$ and $Q1e = 1$
P2c, Q2c	Percentage of constant current impedance with $P1e = 2$ and $Q1e = 2$
P3, Q3	Percentage of constant power load
Pf, Qf	Fraction of static load that is frequency dependent
Df	Frequency dependency factor

B
RULES OF ASSOCIATION

Table B-1
LCET rules of association for downtown commercial building loads

End Use	Motor A	Motor B	Motor C	Motor D	pe	z	i	p
Computer Use	0	0	0	0	1	0	0	0
Cooking	0	0	0	0	0	1	0	0
Cooling	0.1325	0.4725	0.1375	0.035	0.2225	0	0	0
Heating	0	0	0	0	0	1	0	0
Lighting	0	0	0	0	0	0	1	0
Miscellaneous Use	0	0	0	0	0.5	0.5	0	0
Office Equipment	0	0	0	0	1	0	0	0
Refrigeration	0.72	0.09	0.09	0.1	0	0	0	0
Ventilation	0	0.57	0	0	0.43	0	0	0
Water Heating	0	0	0	0	0	1	0	0

Table B-2
LCET rules of association for all commercial loads except downtown building loads

End Use	Motor A	Motor B	Motor C	Motor D	pe	z	i	p
Computer Use	0	0	0	0	1	0	0	0
Cooking	0	0	0	0	0	1	0	0
Cooling	0.65	0.05	0.1	0	0.2	0	0	0
Heating	0	0	0	0	0	1	0	0
Lighting	0	0	0	0	0	0	1	0
Miscellaneous Use	0	0	0	0	0.5	0.5	0	0
Office Equipment	0	0	0	0	1	0	0	0
Refrigeration	0.8	0.1	0.1	0	0	0	0	0
Ventilation	0	0.7	0	0	0.3	0	0	0
Water Heating	0	0	0	0	0	1	0	0

Table B-3
LCET rules of association for residential loads

End use	Motor A	Motor B	Motor C	Motor D	pe	z	i
Clothes Dryer	0	0	0.4	0	0	0.6	0
Cooking	0	0	0	0	0	1	0
Cooling	0	0.1	0.1	0.8	0	0	0
Dishwasher	0	0.5	0	0	0	0.5	0
Freezer	0	0	0	1	0	0	0
Furnace Fans	0	1	0	0	0	0	0
Heating	0	0	0	0.1	0	0.9	0
Lighting	0	0	0	0	0	1	0
Other	0	0	0	0	0.5	0.5	0
Hot Tubs and Spas	0	0	1	0	0	0	0
Pool Pumps and Filters	0	0	1	0	0	0	0
Personal Computers	0	0	0	0	1	0	0
Refrigeration	0	0	0	1	0	0	0
Television	0	0	0	0	1	0	0
Water Heating	0	0	0	0	0	1	0

Table B-4
LMDT rules of association for al commercial loads except downtown office or lodging

End Use	Motor A	Motor B	Motor C	Motor D	pe	z	i
Heating	0	0	0	0	0	1	0
Cooling	0.65	0.05	0.1	0	0.2	0	0
Vent	0	0.7	0	0	0.3	0	0
WaterHeat	0	0	0	0	0	1	0
Cooking	0	0	0	0	0	1	0
Refrig	0.8	0.1	0.1	0	0	0	0
ExtLight	0	0	0	0	0	0	1
IntLight	0	0	0	0	0	0	1
OfficeEquip	0	0	0	0	1	0	0
Misc	0	0	0	0	0	1	0
Process	0	0.3	0	0	0.3	0.4	0
Motors	0	1	0	0	0	0	0
AirComp	1	0	0	0	0	0	0

Table B-5
LMDT rules of association for commercial loads in WECC

End Use	Motor A	Motor B	Motor C	Motor D	pe	z	i
Heating	0.3					0.7	
Cooling	0.65	0.05	0.1		0.2		
Vent		0.7			0.3		
WaterHeat						1	
Cooking		0			0	1	
Refrig	0.8	0.1	0.1				
ExtLight							1
IntLight							1
OfficeEquip					1		
Misc					1		
Process		0.3	0.2		0.5		
Motors		0.5	0.5				
AirComp	1						

Table B-6
LMDT rules of association for residential feeders in WECC

End Use	Motor A	Motor B	Motor C	Motor D	Motor A	Z	I
Heating				0.3		0.7	
Cooling		0.1		0.85	0.05		
Vent		1					
WaterHeat						1	
Cooking		0.15				0.85	
Refrig				1			
ExtLight						1	
IntLight						1	
Electronics					1		
Appliances			0.2		0.1	0.7	
Misc			0.3		0.2	0.5	
Vehicle					1		

The Electric Power Research Institute, Inc. (EPRI, www.epri.com) conducts research and development relating to the generation, delivery and use of electricity for the benefit of the public. An independent, nonprofit organization, EPRI brings together its scientists and engineers as well as experts from academia and industry to help address challenges in electricity, including reliability, efficiency, affordability, health, safety and the environment. EPRI also provides technology, policy and economic analyses to drive long-range research and development planning, and supports research in emerging technologies. EPRI members represent 90% of the electricity generated and delivered in the United States with international participation extending to nearly 40 countries. EPRI's principal offices and laboratories are located in Palo Alto, Calif.; Charlotte, N.C.; Knoxville, Tenn.; Dallas, Texas; Lenox, Mass.; and Washington, D.C.

Together…Shaping the Future of Electricity

3002019209

Electric Power Research Institute
3420 Hillview Avenue, Palo Alto, California 94304-1338 • PO Box 10412, Palo Alto, California 94303-0813 • USA
800.313.3774 • 650.855.2121 • askepri@epri.com • www.epri.com